Supplemental Information

Aqp2^{+} progenitor cells maintain and repair distal renal segments

Chao Gao, Long Zhang[$], Enuo Chen, Wenzheng Zhang[*]

Department of Regenerative & Cancer Cell Biology, Albany Medical College, Albany, NY 12208

[*]Correspondence: zhangw1@mail.amc.edu.

$Current address: Pulmonary and Critical Care Medicine, Harvard Medical School.

This PDF file includes:

Supplementary Methods and Discussion

Table S1-S7

Figures S1 to S22

Movie S1

References for SI

Supplementary Results and Discussion

Supplemental Table S1-S6, Figures S1-S22, and Movies S1.

Table S1. Abbreviations

Table S2. $Aqp2^+$ cells to $B1B2^+$ cell conversion percentage and $Aqp2^+$ cell-derived $B1B2^+$ cell percentage

Table S3. $Aqp2^+$ cells to NCC^+ cell conversion percentage and $Aqp2^+$ cell-derived NCC^+ cell percentage

Table S4. $Aqp2^+$ cells to $CAII^+$ cell conversion percentage and $Aqp2^+$ cell-derived $CAII^+$ cell percentage

Table S5. $Aqp2^+$ cells to $AE1^+$ cell conversion percentage and $Aqp2^+$ cell-derived $AE1^+$ cell percentage

Table S6. $Aqp2^+$ cells to $Pendrin^+$ cell conversion percentage and $Aqp2^+$ cell-derived $Pendrin^+$ cell percentage

Table S7. $Aqp2^+$ cells to $B1B2^+$ cell conversion percentage and $Aqp2^+$ cell-derived $B1B2^+$ cell percentage at D6 post UUO

Figure S1. $Aqp2^+$ $B1B2^+$ and $Aqp2^+$ $B1^+$ cells with and without detectable expression of Aqp3 and Aqp4 exist in E15.5 kidneys.

Figure S2. $Aqp2^+$ $B1B2^+$ cells with and without detectable expression of other PC and IC markers exist in adult WT C57Bl/6 kidneys.

Figure S3. $Aqp2^+$ $B1^+$ cells with and without detectable expression of other PC and IC markers exist in adult kidneys

Figure S4. No converted IC and DCT2 cells in adult $Aqp2^{ECE/+}$ *RFP/+* mice one day after Tamoxifen induction.

Figure S5. Converted B1B2^{+} and CAII^{+} cells in adult *Aqp2$^{ECE/+}$ RFP/+* mice 300 days after Tamoxifen induction.

Figure S6. Converted AE1^{+} and Pendrin^{+} cells in adult *Aqp2$^{ECE/+}$ RFP/+* mice 300 days after Tamoxifen induction.

Figure S7. Converted B1^{+} (Aqp2^{-}B1^{+}RFP^{+}) cells in adult *Aqp2$^{ECE/+}$ RFP/+* mice 300 days after Tamoxifen induction.

Figure S8. Optimization of Tamoxifen induction and validation of the lack of cross reactivity between the GFP and RFP antibodies in adult *Aqp2$^{ECE/+}$ Brainbow/+* mice.

Figure S9. Individual XFP^{+} cells in adult *Aqp2$^{ECE/+}$ Brainbow/+* mice one day post 1X 2 mg Tamoxifen induction.

Figure S10. Validation of specific detection of XFP on paraffin sections.

Figure S11. No converted GYC^{+} cells in adult *Aqp2$^{ECE/+}$ Brainbow/+* mice one day post induction.

Figure S12. RFP^{+} clones containing 1-3 cells in adult *Aqp2$^{ECE/+}$ Brainbow/+* mice 30 days post induction.

Figure S13. Adult AP express Jag1 and Notch1.

Figure S14. Adult AP express CD24 and Pax2.

Figure S15. Adult AP express Parm1 and lack detectable Ki67 and PCNA.

Figure S16. Adult AP occasionally and selectively divide during renal maintenance.

Figure S17. Validation of specific detection of CldU and IdU.

Figure S18. UUO-induced injury repair involves specific CNT/CD cells as the first responders.

Figure S19. Adult AP selectively proliferate in response to UUO-induced injury at D2.

Figure S20. Adult AP exist in the expanded CldU^{+} clones.

Figure S21. Sparsely distributed individual XFP^{+} cells in the adult *Aqp2$^{ECE/+}$ Brainbow/Brainbow* mice 24h post Tamoxifen induction without UUO.

Figure S22. RFP^{+} clones of 1-2 cells in the adult *Aqp2$^{ECE/+}$ Brainbow/Brainbow* mice at D14 without UUO.

Figure S23. Adult AP express Jag1 and Notch1 during repair.

Figure S24. Notch is activated during repair

Figure S25. UUO progressively induces kidney fibrosis.

Movie S1. Adult AP contribute circumferentially and longitudinally to CNT/CD maintenance.

References

Supplementary Results and Discussion

Adult AP express Jag1 and Notch 1. Embryonic AP express IC-selective Notch ligand Jag1, and PC-selective Notch receptor Notch1. The putative markers of renal progenitor cells (Pax2, CD24, and CD133) were also detectable in embryonic AP [1]. All of these molecules except CD133 were also discerned in adult AP as well as in PC or IC (Figure S10-11). CD133 was barely detectable in CNT/CD cells despite its high expression in $Aqp2^-$ tubules (Figure S11B). Based on single-cell RNA-Seq analyses and IF, Parm1 was proposed as a marker of cells expressing Aqp2 and V-ATPase subunit B1 ($Aqp2^+$ $B1^+$) in adult mouse kidney [2]. Nevertheless, with the same Parm1 antibody used in [2], we detected Parm1 in AP and some PC and IC (Figure S12A). Most, if not all adult AP, like PC and IC, had undetectable Ki67 and PCNA (Figure S12B-C).

We did not use the multiple-cell/(single-cell + multiple-cell) clone ratio to estimate the relative abundance of AP during renal maintenance for 3 reasons: 1) Renal epithelia are completely renewed 4.6-6 times over 7 months in adult mouse kidney [3], although it is unclear if all renal epithelial cells renew at the same rate. The initially-labeled regular PC are likely to have been replaced by daughter cells derived from AP. Hence, even single XFP^+ cells post extended induction could be offspring of AP. 2) Additional XFP^+ cells may appear in different confocal planes ([4] and Figure 2E-F); and 3) *Aqp2*$^{ECE/+}$ *Brainbow/+* mice yield XFP^+ cells primarily in inner medulla and rarely in the cortex (Fig. 2B), this biased labeling efficiency makes it impractical to accurately estimate the percentage of AP in the whole kidney. Circulating cells are very unlikely to contribute to adult DCT2, CNT and CD maintenance because of their

negligible contributions to kidney maintenance and inability to incorporate into any glomerular, tubular or vascular structures [3].

Single cell RNA-Seq revealed Parm1 as cell-specific markers of the aforementioned cluster 8 [2]. Our IF with the same anti-Parm1 antibody showed that Parm1 is not only detectable in AP, but also in some PC and IC (Figure S12A). What contributes to this discrepancy remains mysterious.

The Notch ligands and receptors can interact both within the same cell (cis) and across cell boundaries (trans). Cis-interactions can inhibit or activate productive signaling. Cis-activation happens for numerous ligand-receptor pairs, in various cell types, and impacts survival in neural stem cells [5]. Co-expression of Jag1 and Notch1 implies that AP have the potential to cis-activate. Self-renewing AP thus can be self-dependent, sending and receiving their own Notch signaling. Consistently, Notch activation correlates with proliferation in AP (Figure 7E). While Notch activation is not associated with proliferation of PC (Figure S22D), it may be required for their fate selection and maintenance [6, 7].

Both thymidine analog labeling and in vivo lineage tracing with *Aqp2*^{ECE} have complementary advantages and limitations, allowing mutual data validation. The analog labeling permits analyses of the cortex, overcoming the limitation of *Aqp2*$^{ECE/+}$ *Brainbow* mice, which were predominantly restricted to the inner medulla. Incorporation of the analogs, however, does not necessarily mean that the cells have indeed divided; they may have also endoreplicated, which means DNA replication without cytokinesis [4]. Although this possibility cannot be conclusively eliminated, single-colored multiple-cell clones derived from the *Brainbow* reporter harbored PC, IC and AP during renal maintenance, and repair (Figure 2E-F and 6B-H). These results

consistently support the notion that a unique, fixed subpopulation of Aqp2$^+$ cells has the self-renewal, clonogenicity, and multipotency. Finally, *Aqp2^{ECE}* presumably allow tracing the lineages of both AP and regular PC. *Aqp2^{ECE}*-based lineage tracing, however, cannot distinguish if conversion occurs in cell division dependent or -independent manners. This limitation is overcome by CIdU labeling (Figure 8).

Table S1. Abbreviations

DCT2	late distal convoluted tubules
CNT	connecting tubules
CD	collecting ducts
B1B2	V-ATPase subunits B1 and B2
CAII	carbonic anhydrase II
PC	principal cells
IC	intercalated cells
AP	$Aqp2^+$ $B1B2^+$ progenitor cells
TC1	putative transitional cells ($Aqp2^+CAII^+$)
TC2	putative transitional cells ($Aqp2^+AE1^+$)
TC3	putative transitional cells ($Aqp2^+Pendrin^+$)
TC4	putative transitional cells ($Aqp2^-$ $B1B2^-$)
TC5	putative transitional cells ($Aqp2^+$ NCC^+)
RFP	red fluorescence protein
GFP	green fluorescence protein
YFP	yellow fluorescence protein
CFP	cyan fluorescence protein
XFP	red, green, yellow and cyan fluorescence proteins
GYC	green, yellow and cyan fluorescence proteins
DAPI	4', 6-diamidino-2-phenylindole
IF	immunofluorescence staining
ECE	conditionally active form of Cre recombinase (activated in

	response to Tamoxifen) encoded by *ER^{T2}CreER^{T2}* cassette
UUO	unilateral ureteral obstruction
CIdU	chlorodeoxyuridine
IdU	idodeoxyuridine

Table S2. Aqp2$^+$ cells to B1B2$^+$ cell conversion percentage and Aqp2$^+$ cell-derived B1B2$^+$ cell percentage during renal maintenance

		Total RFP$^+$	Total B1B2$^+$	Aqp2$^-$ RFP$^+$ B1B2$^+$	Aqp2$^-$ RFP$^+$ B1B2$^+$/ Total RFP$^+$ (%)	Aqp2$^-$ RFP$^+$ B1B2$^+$/ Total B1B2$^+$ (%)
D1	Cortex	1300	880	0	0.00	0.00
	Outer Medulla	1910	710	0	0.00	0.00
	Inner Medulla	1800	680	0	0.00	0.00
D60	Cortex	2680	1954	125	4.66	6.40
	Outer Medulla	5696	2064	27	0.47	1.31
	Inner Medulla	5823	2183	23	0.39	1.05
D90	Cortex	2578	1915	138	5.35	7.21
	Outer Medulla	4742	1813	32	0.67	1.77
	Inner Medulla	5310	2678	26	0.49	0.97
D300	Cortex	2766	1417	459	16.59	32.39
	Outer Medulla	4232	1492	101	2.39	6.77
	Inner Medulla	4472	1894	48	1.07	2.53

Table S3. Aqp2$^+$ cells to NCC$^+$ cell conversion percentage and Aqp2$^+$ cell-derived NCC$^+$ cell percentage during renal maintenance

		Total RFP$^+$	Total NCC$^+$	Aqp2$^-$ RFP$^+$ NCC$^+$	Aqp2$^-$ RFP$^+$ NCC$^+$/ Total RFP$^+$ (%)	Aqp2$^-$ RFP$^+$ NCC$^+$/ Total NCC$^+$ (%)
D1	Cortex	2000	30000	0	0.00	0.00
D60	Cortex	10450	195400	4	0.038	0.002
D90	Cortex	10770	209000	5	0.046	0.002
D300	Cortex	5520	88200	5	0.091	0.006

Table S4. Aqp2$^+$ cells to CAII$^+$ cell conversion percentage and Aqp2$^+$ cell-derived CAII$^+$ cell percentage during renal maintenance

		Total RFP$^+$	Total CAII$^+$	Aqp2$^-$ RFP$^+$ CAII$^+$	Aqp2$^-$ RFP$^+$ CAII$^+$/ Total RFP$^+$ (%)	Aqp2$^-$ RFP$^+$ CAII$^+$/ Total CAII$^+$ (%)
D1	Cortex	1030	850	0	0.00	0.00
	Outer Medulla	1100	260	0	0.00	0.00
	Inner Medulla	1250	180	0	0.00	0.00
D60	Cortex	2156	1712	132	6.12	7.71
	Outer Medulla	1145	244	5	0.44	2.05
	Inner Medulla	1294	205	4	0.31	1.95
D90	Cortex	2223	1540	113	5.08	7.34
	Outer Medulla	1567	329	7	0.45	2.13
	Inner Medulla	2111	400	6	0.28	1.50
D300	Cortex	1264	885	370	29.27	41.81
	Outer Medulla	2260	800	67	2.96	8.38
	Inner Medulla	1000	333	17	1.70	5.11

Table S5. Aqp2$^+$ cells to AE1$^+$ cell conversion percentage and Aqp2$^+$ cell-derived AE1$^+$ cell percentage during renal maintenance

		Total RFP$^+$	Total AE1$^+$	Aqp2$^-$ RFP$^+$ AE1$^+$	Aqp2$^-$ RFP$^+$ AE1$^+$/ Total RFP$^+$ (%)	Aqp2$^-$ RFP$^+$ AE1$^+$/ Total AE1$^+$ (%)
D1	Cortex	1050	456	0	0.00	0.00
	Outer Medulla	2122	690	0	0.00	0.00
	Inner Medulla	1500	510	0	0.00	0.00
D60	Cortex	2175	905	77	3.54	8.51
	Outer Medulla	4165	1395	45	1.08	3.23
	Inner Medulla	1450	450	9	0.62	2.00
D90	Cortex	2324	956	85	3.66	8.89
	Outer Medulla	2783	1029	33	1.19	3.21
	Inner Medulla	1711	491	11	0.64	2.24
D300	Cortex	1079	688	266	24.65	38.66
	Outer Medulla	1500	600	54	3.60	9.00
	Inner Medulla	557	350	11	1.97	3.14

Table S6. Aqp2$^+$ cells to Pendrin$^+$ cell conversion percentage and Aqp2$^+$ cell-derived Pendrin$^+$ cell percentage during renal maintenance

		Total RFP$^+$	Total Pendrin$^+$	Aqp2$^-$ RFP$^+$ Pendrin$^+$	Aqp2$^-$ RFP$^+$ Pendrin$^+$/ Total RFP$^+$ (%)	Aqp2$^-$ RFP$^+$ Pendrin$^+$/ Total Pendrin$^+$ (%)
D1	Cortex	2105	823	0	0.00	0.00
D60	Cortex	2410	925	110	4.56	11.89
D90	Cortex	1953	800	96	4.92	12.00
D300	Cortex	500	279	112	22.40	40.14

Table S7. Aqp2$^+$ cells to B1B2$^+$ cell conversion percentage and Aqp2$^+$ cell-derived B1B2$^+$ cell percentage at D6 post UUO

		Total RFP$^+$	Total B1B2$^+$	Aqp2$^-$ RFP$^+$ B1B2$^+$	Aqp2$^-$ RFP$^+$ B1B2$^+$/ total RFP$^+$ (%)	Aqp2$^-$ RFP$^+$ B1B2$^+$/ total B1B2$^+$ (%)
D6	Cortex	1323	689	70	5.3	10
	Outer Medulla	1262	224	14	1.1	6.3
	Inner Medulla	1147	301	11	1	3.7

Figure S1. Aqp2$^+$ B1B2$^+$ and Aqp2$^+$ B1$^+$ cells with and without detectable expression of Aqp3 and Aqp4 exist in E15.5 kidneys.

(A-B) Images of Aqp2 (blue) merged with DAPI (white), B1B2 (green), and Aqp3 (A) or Aqp4 (B) (both in red) in E15.5 kidneys showing that some AP expressed Aqp3 and/or Aqp4 while others lacked detectable Aqp3 and/or Aqp4. Images in the inserts were from different regions of E15.5 kidneys. Arrowheads: AP were magnified 2.3X on the far right lacking or expressing Aqp3 or Aqp4.

(C-D). As in A-B, except B1B2 replaced with B1, which is merged with DAPI. Images in the inserts were from different regions of E15.5 kidneys.

Scale bar: 50 μm. Related to Figures 1 and 2.

Figure S2. Aqp2$^+$ B1B2$^+$ cells with and without detectable expression of other PC and IC markers exist in adult WT C57Bl/6 kidneys.

(A-B) Images of Aqp2 (blue) merged with DAPI (white), B1B2 (green), and Aqp3 (A) or Aqp4 (B) (both in red) in adult WT C57Bl/6 kidneys. Images in the inserts in each panel were from different regions of the same sections. Arrowheads: AP were magnified 2.3X on the far right lacking or expressing Aqp3 or Aqp4.

(C-E) As in A, except Aqp3 replaced with X (X=CAII, AE1, or Pendrin as indicated), and B1B2 merged with DAPI. Images in the inserts in each panel were from different regions of the same sections.

Scale bar: 50 μm. Related to Figures 1 and 2.

Figure S3. Aqp2$^+$ B1$^+$ cells with and without detectable expression of other PC and IC markers exist in adult kidneys.

(A-E) Images of Aqp2 (blue), B1 (green) merged with DAPI (white), and X (red, X=Aqp3, Aqp4, CAII, AE1, or Pendrin) in adult WT C57Bl/6 kidneys. Images in the inserts in A and B were from different regions of the same sections. In D, both rabbit B1 and AE1 primary antibodies were used sequentially in combination of monovalent Fab fragments of secondary antibodies (see Immunofluorescence studies in Methods section). Arrowheads: AP were magnified 2.3X on the far right lacking or expressing X (X= Aqp3, Aqp4, CAII, AE1, or Pendrin). Scale bar: 50 μm. Related to Figures 1 and 2.

Figure S4. No converted IC and DCT2 cells in adult *Aqp2$^{ECE/+}$ RFP/+* mice one day after Tamoxifen induction.

(A) RFP expression in the Aqp2^{+} lineage after Tamoxifen induced ECE-mediated recombination in *Aqp2$^{ECE/+}$ RFP/+* mice. .

(B) *Adult Aqp2$^{ECE/+}$ RFP/+* mice were injected with 1 X 2 mg Tamoxifen at day 0 and examined at day 1 post induction (D1).

(C-G) Immunofluorescence confocal images of Aqp2 (white), RFP (red), X (green, X = V-ATPase B1B2, CAII, AE1, Pendrin, and NCC), and DAPI (blue) in adult *Aqp2$^{ECE/+}$ RFP/+* kidneys at day 1 post 1 X 2 mg Tamoxifen induction. Boxed areas were magnified 2X on the right, with channels split. Scale bar: 50 μm. Arrowhead: cells were magnified 4X in inserts, highlighting no conversion of Aqp2^{+} cells into IC or DCT2 cells during a short time period after Tamoxifen induction as detailed below.

(C) No converted Aqp2^{-} RFP^{+} B1B2^{+} cells, despite existence of rare labeled AP (Aqp2^{+} B1B2^{+} RFP^{+})

(D) No converted Aqp2^{-} RFP^{+} CAII^{+} cells.

(E) No converted Aqp2^{-} RFP^{+} AE1^{+} cells.

(F) No converted Aqp2^{-} RFP^{+} Pendrin^{+} cells.

(G) No converted Aqp2^{-} RFP^{+} NCC^{+} cells.

Related to Figure 1.

Figure S5. Converted B1B2^{+} and CAII^{+} cells in adult *Aqp2$^{ECE/+}$ RFP/+* mice 300 days after Tamoxifen induction.

(A) Adult *Aqp2$^{ECE/+}$ RFP/+* mice were injected with 1 X 2 mg Tamoxifen at day 0 and examined at day 300 post induction (D300).

(B-F) Immunofluorescence confocal images of Aqp2 (blue), X (green, X = B1B2 (B, & C) or CAII (D-F), and RFP (red)) in the regions as indicated in *Aqp2$^{ECE/+}$ RFP/+* kidneys at day 300. Arrows: converted cells were magnified 4X in insets and detailed below.

(B-C) Converted Aqp2^{-} RFP^{+}CAII^{+} cells.

(D-F) Converted Aqp2^{-} RFP^{+}CAII^{+} cells.

Arrowheads in E: TC1 (Aqp2^{+}CAII^{+})

Scale bar: 50 μm. Related to Figures 1.

Figure S6. Converted AE1^{+} and Pendrin^{+} cells in adult *Aqp2$^{ECE/+}$ RFP/+* mice 300 days after Tamoxifen induction.

(A) Adult *Aqp2$^{ECE/+}$ RFP/+* mice were injected with 1 X 2 mg Tamoxifen at day 0 and examined at day 300 post induction (D300).

(B-E) Immunofluorescence confocal images of Aqp2 (blue), X (green, X = AE1 (B-D) or Pendrin (E), and RFP (red)) in the regions as indicated in *Aqp2$^{ECE/+}$ RFP/+* kidneys at day 300. Arrows: converted cells were magnified 4X in insets and detailed below.

(B-D) Converted Aqp2^{-}RFP^{+}AE1^{+} cells.

(E) Converted Aqp2^{-}RFP^{+}Pendrin^{+} cells.

Scale bar: 50 μm. Related to Figures 1.

Figure S7. Converted B1$^+$ (Aqp2$^-$B1$^+$RFP$^+$) cells in adult *Aqp2$^{ECE/+}$ RFP/+* mice 300 days after Tamoxifen induction.

Immunofluorescence confocal images of Aqp2 (blue), B1 (green) merged with DAPI (white) and RFP (red)) in *Aqp2$^{ECE/+}$ RFP/+* kidneys at day 300. Arrows: a converted B1 cell (Aqp2$^-$ B1$^+$RFP$^+$ was magnified 4X in insets.

Figure S8. Optimization of Tamoxifen induction and validation of the lack of cross reactivity between the GFP and RFP antibodies in adult *Aqp2$^{ECE/+}$ Brainbow/+* mice.

(A-C) Adult *Aqp2$^{ECE/+}$ Brainbow/+* mice were induced with 1 X 2 mg Tamoxifen at D0 and analyzed at D1. Immunofluorescence confocal images of Aqp2 (blue) merged with DAPI (white), RFP (red), and GFP (green) showed individual RFP$^+$ and GYC$^+$ cells primarily in the inner medulla, occasionally in the outer medulla and very rarely in the cortex. The non-overlapping detection of RFP$^+$ and GYC$^+$ cells demonstrated the lack of cross reactivity between the GFP and RFP antibodies.

(D-F) Adult *Aqp2$^{ECE/+}$ Brainbow/+* mice were induced daily with 5 X 5 mg Tamoxifen at D0-D5 and analyzed at D6. Immunofluorescence confocal images of Aqp2 (red), GFP (green) and DAPI (blue) showed GYC$^+$ “clones” with various numbers of cells primarily in the inner medulla, occasionally in the outer medulla and very rarely in the cortex.

(G) Adult *Aqp2$^{ECE/+}$ Brainbow/+* mice were induced with 1 X 2 mg oil at D0 and analyzed at D1. Immunofluorescence confocal images of Aqp2 (red), GFP (green) and DAPI (blue) showed no GYC$^+$ cells in the inner medulla.

Scale bar: 50 μm. Related to Figure 2.

Figure S9. Individual XFP$^+$ cells in adult *Aqp2$^{ECE/+}$ Brainbow/+* mice one day post 1X 2 mg Tamoxifen induction.

(A) Adult *Aqp2$^{ECE/+}$ Brainbow/+* mice were induced with 1 X 2 mg Tamoxifen at D0 and analyzed at D1. Frozen sections without immunofluorescence staining were subject to confocal microscopy.

(B-C) Images of frozen sections showing sparsely distributed XFP$^+$ cells primarily in the inner medulla. Boxed area was magnified 4X in C. No antibody staining was involved.

(D) 100% XFP$^+$ clones contained only one cell. No XFP$^+$ clones had 2 or more XFP$^+$ cells. A total of 1001 clones from 3 mice were examined.

Scale bar: 50 μm. Related to Figure 2.

Figure S10. Validation of specific detection of XFP on paraffin sections.

(A) Adult *Aqp2$^{ECE/+}$ Brainbow/+* mice were induced with 1 X 2 mg Tamoxifen at D0 and analyzed at D300 for immunofluorescence staining of paraffin sections without primary antibodies or using normal mouse and rabbit IgGs.

(B) Confocal images showed no XFP$^+$ cells when the primary antibodies were omitted. Boxed area was magnified 2X on the right.

(C) Confocal images of Aqp2 (blue) merged with DAPI (white, left), or with normal mouse IgG (mIgG, green) and normal rabbit IgG (rIgG, red) showed no XFP$^+$ cells. In either case, no XFP$^+$ cells were detected, demonstrating the disruption of green, red, yellow and cyan-emitting fluorophores by the immunofluorescence staining procedure and the dependence of the primary antibodies for the detection of XFP.

Scale bar: 100 μm. Related to Figure 2.

Figure S11. No converted GYC$^+$ cells in adult *Aqp2$^{ECE/+}$ Brainbow/+* mice one day post induction.

(A-F) Immunofluorescence confocal images of Aqp2 (blue) merged with DAPI (white), X (X= B1B2, CAII, AE1, and Pendrin, all in red) and GYC recognized by the GFP antibody (green) showing that individual GYC$^+$ (green) cells expressing Aqp2 with or without X throughout the Aqp2$^{ECE/+}$ *Brainbow/+* kidneys 1 day after 1 X 2 mg Tamoxifen injection. Arrowheads: Individual GYC$^+$ cells magnified 4X in inserts are either AP or Aqp2$^+$X$^-$ cells, demonstrating no Aqp2$^+$ cells to X$^+$ conversion as detailed below. Scale bar: 50 μm.

(A) Labeled Aqp2$^+$ B1B2$^+$ GYC$^+$ cells (i.e. Labeled AP).

(B-C) No converted Aqp2$^-$ B1B2$^+$ GYC$^+$ cells in the outer (B) and inner medulla (C).

(D) No converted Aqp2$^-$ CAII$^+$ GYC$^+$ cells in the inner medulla.

(E) No converted Aqp2$^-$ AE1$^+$ GYC$^+$ cells in the inner medulla.

(F) A very rare GYC$^+$ cell in the cortex that was Aqp2$^+$ Pendrin$^-$.

Related to Figure 2.

Figure S12. RFP$^+$ clones containing 1-3 cells in adult *Aqp2$^{ECE/+}$ Brainbow/+* mice 30 days post induction.

(A) Adult *Aqp2$^{ECE/+}$ Brainbow/+* mice were induced with 1 X 2 mg Tamoxifen at D0 and analyzed at D30.

(B-C) Immunofluorescence confocal images of Aqp2 (green), RFP (red) and DAPI (blue) showed RFP$^+$ "clones" with 1-3 cells in the inner medulla. Boxed area was magnified 4X in C.

(D) Percent of XFP$^+$ clones showing that 99.4% XFP$^+$ clones had 1-2 cells. The remaining 0.6% clones had 3 cells XFP$^+$ clones. No XFP$^+$ clones had 4 or more XFP$^+$ cells. A total of 1203 clones from 3 mice were examined. Scale bar: 50 μm. Related to Figure 2.

Figure S13. Adult AP express Jag1 and Notch1.

(A-B) Images of Aqp2 (blue) merged with DAPI (white), B1B2 (green), and X (X=Jag1 or Notch, both in red) in adult WT C57Bl/6 kidneys showing that AP express Jag1 and Notch1. Notch1 and Jag1 were also expressed in PC and IC, respectively. The 4th row of small enlarged panels at the right of each lettered subpanel presents the Aqp2/B1B2/X merged image. Scale bar: 50 μm. Related to Figures 1 and 2.

Figure S14. Adult AP express CD24 and Pax2.

(A-B) Images of Aqp2 (blue) merged with DAPI (white), B1B2 (green), and X (X=CD24, or Pax2, both in red) in adult WT C57Bl/6 kidneys showing that AP, like PC and IC, express CD24 and Pax2,. The 4th row of small enlarged panels at the right of each lettered subpanel presents the Aqp2/B1B2/X merged image. Scale bar: 50 μm. Related to Figures 1 and 2.

Fig. S15. Adult AP express Parm1, but not Ki67 and PCNA.

(A-C) Images of Aqp2 (blue) merged with DAPI (white), B1B2 (green), and X (X=Parm1, Ki67 or PCNA, all in red) in adult WT C57Bl/6 kidneys showing that AP, like PC and IC, express Parm1, but neither Ki67 nor PCNA. The 4th row of small enlarged panels at the right of each lettered subpanel presents the Aqp2/B1B2/X merged image. Scale bar: 50 μm. Related to Figures 1 and 2.

Figure S16. Adult AP occasionally and selectively divide during renal maintenance.

(A) Adult WT mice were injected with CldU (50 mg/kg BW) at 0h without UUO. Mice were analyzed at 24h.

(B) Percent of various CNT/CD cells: PC ($Aqp2^+$ $B1B2^-$), IC ($Aqp2^-$ $B1B2^+$), AP ($Aqp2^+$ $B1B2^+$), and TC4 ($Aqp2^-$ $B1B2^-$) throughout the kidney. A total of 5520 cells from 3 mice were counted and classified into PC, IC, AP or TC4. Error bars represent ± SEM.

(C) Percent of CldU-labeled various CNT/CD cells throughout the kidney. A total of 5520 cells from 3 mice were counted and classified into PC, IC, AP or TC4. For each cell type, cells were then scored as $CldU^+$ and $CldU^-$, respectively (see text for details). Error bars represent ± SEM.

(D-E) Matched immunofluorescence confocal images of Aqp2 (blue) merged with B1B2 (green) and CldU (red, D), or with DAPI (white, E) in the chased kidney. Boxed area in D was matched with boxed area in E, and magnified 4.5X in F, highlighting a 2-cell $CldU^+$ clone containing an AP ($Aqp2^+$ $B1B2^+$) and IC ($Aqp2^-$ $B1B2^+$), with separated channels. No other $CldU^+$ CNT/CD cells were found throughout the image (D-E). Arrows and arrowheads in D & E: All other $CldU^+$ cells in $Aqp2^-$ tubules and interstitial structures, respectively. Arrows in F: The 2-cell $CldU^+$ clone magnified 2,5X in G. Scale bar: 50 μm.

Figure S17. Validation of specific detection of CldU and IdU.

(A) Adult mice were subject to UUO at 0h, followed by injection of CldU, IdU or in combination (50 mg/kg BW each), respectively, at 24h post UUO. For combinational injection, IdU was injected at 45h post UUO. Mice were analyzed at 48h.

(B-D) Images showing CldU (red) and IdU (green) labeling in the kidneys. When either CldU (B) or IdU (C) was administrated alone no cross-reactivity was detected, and when both CldU and IdU (D) were sequentially injected, cells labeled by CldU, IdU or both were found. Scale bar: 50 μm. Arrowheads: Cells were magnified 4X in inserts. Arrow in D: $CldU^+$ or IdU^+ cells. Related to Figures 3-5, and 7.

Figure S18. UUO-induced injury repair involves specific CNT/CD cells as the first responders.

(A) Adult mice were subject to UUO, and injected with CldU 24h after injury and IdU at 45h after injury. Mice were sacrificed at 48h or day 14 (14d) post-UUO.

(B-D) Immunofluorescence confocal images of Ki67 (blue), CldU (red), IdU (green) and DAPI (white) in UUO kidneys at 48h. The boxed area in B was matched with boxed area in C and magnified 6X in D with separated channels. The 4th panel in D presents the Ki67/CldU/IdU merged image.

(E) Percent of Ki67$^+$ cells in CldU$^+$IdU$^+$ cells (left, green) and CldU$^+$IdU$^+$ cells in Ki67$^+$ cells (right, green) in UUO kidneys at 48h. The red portions of bars show percent of Ki67$^-$ cells in CldU$^+$IdU$^+$ cells (left), and percent of CldU$^-$, IdU$^-$, or CldU$^-$IdU$^-$ cells in Ki67$^+$ cells (right) in UUO kidneys at 48h. From 3 mice, 500 CldU$^+$IdU$^+$ and 801 Ki67$^+$ cells were counted.

(F-K) Immunofluorescence confocal images of Aqp3 (blue), CldU (red), TUNEL (green) and DAPI (white) in UUO kidneys at 48h. Boxed regions in F were matched with boxed areas in I, and magnified 3X to highlight that injured CNT/CDs either containing apoptotic cells had (G and J) or lacked (H and K) CldU$^+$ cells. Arrowheads: apoptotic cells.

(L-O) Immunofluorescence confocal images of Aqp3 (blue), CldU (red), TUNEL (green) and DAPI (white) in UUO kidneys at 14d. Injured CNT/CDs containing apoptotic cells either lacked (L and N) or had (M and O) CldU$^+$ cells, respectively. Arrowheads: apoptotic cells.

Scale bar: 50 μm. Related to Figure 3-4.

Figure S19. Adult AP selectively proliferate in response to UUO-induced injury at D2.

(A-B) Adult WT mice were subject to UUO at day 0 (d0), CldU injection at day 1 (D1), and examined at 2 days later (D2). Matched images of Aqp2 (green), B1B2 (red) merged with DAPI (white), and CldU (blue) showing two adjacent labeled AP (Aqp2$^+$ B1B2$^+$ CldU$^+$) in the boxed

region as the sole CIdU$^+$ CNT/CD cells in the whole area examined, demonstrating the selective proliferation of AP in UUO kidneys at D2. Boxed areas in A and B were matched and magnified 8X in Figure 4F. No other CIdU$^+$ CNT/CD cells were found throughout the images in A and B.

Figure S20. Adult AP exist in the expanded CIdU$^+$ clones.

(A) Adult mice were subject to UUO at d0, followed by CIdU injection at D1, and examined at D6.

(B-D) Images of three confocal planes from the top to the bottom showing the same CIdU-labeled CNT/CD in a UUO kidney, with Aqp2 (blue), B1B2 (green) merged with DAPI (white), and CIdU (red). Arrowheads: AP (B & C) and PC (D) were magnified 2.3X in far right, highlighting the lack of AP detection in the CIdU$^+$ clone (D) because AP resides in different confocal planes (B & C). Scale bar: 50μm. Related to Figure 4.

Figure S21. Sparsely distributed individual XFP$^+$ cells were induced in the adult *Aqp2$^{ECE/+}$ Brainbow/Brainbow* mice.

(A) Adult *Aqp2$^{ECE/+}$ Brainbow/Brainbow* mice were induced with 1 X 2 mg Tamoxifen at D0 and sacrificed 24hrs later (D1) without UUO for confocal microscopy of frozen sections.

(B-C) Images of frozen sections of adult *Aqp2$^{ECE/+}$ Brainbow/Brainbow* mice at D1 showing sparsely distributed individual XFP-labeled cells (X=G, Y, C and R). Boxed area in B is magnified 4X to highlight individual XFP$^+$ cells in the inner medulla (C)**.** No antibody staining was involved. n=3 mice.

(D) Percent of XFP$^+$ clones containing 1, 2 or more continuous XFP$^+$ cells of the same color without interruption by an unlabeled cell or by a cell labeled by a different color at D1. Clones of 2 or more XFP$^+$ cells were not found. A total of 1105 clones from 3 mice were analyzed.

Scale bar: 50 μm. Related to Figure 6.

Figure S22. RFP$^+$ clones with 1-2 cells were induced in the adult *Aqp2$^{ECE/+}$ Brainbow/Brainbow* mice at D14.

(A) Adult *Aqp2$^{ECE/+}$ Brainbow/Brainbow* mice were induced with 1 X 2 mg Tamoxifen at D-1, without UUO at d0, and sacrificed at D14 as non-injured control. The time points were matched with the UUO mice at D14 shown in Figure 6.

(B-C) Immunofluorescence confocal images of Aqp2 (green), RFP (red) and DAPI (blue) showed RFP$^+$ "clones" with 1-2 cells in the inner medulla. Boxed area was magnified 4X in C.

(D) Percent of XFP$^+$ clones showing that 100% XFP$^+$ clones had 1-2 cells. Clones of 3 or more XFP$^+$ cells were not observed. A total of 605 clones from 3 mice were analyzed.

Scale bar: 50 μm. Related to Figure 6.

Figure S23. Adult AP express Jag1 and Notch1 during repair.

(A) Adult mice were subject to UUO at day 0 (d0), CldU injection at day 1 (D1), and examined 2, 6 or 14 days later (D2, D6, or D14).

(B) Mice were injected with CIdU and sacrificed one day later as non-injured control (D0).

(C-H) Immunofluorescence images of UUO kidneys showing Aqp2 (green) merged with DAPI (white), or with B1B2 (red) and Jag1 or Notch1 (blue) as indicated. Arrowheads: AP (Aqp2$^+$ B1B2$^+$) were magnified 2.3X on the far right.

(C, E, G) AP expressed high levels of Jag1.

(D, F, H) AP expressed high levels of Notch1.

(I-J) Percent of AP expressing Jag1 (I) or Notch1 (J) in all AP at each time point. About 300 AP were counted per condition. Scale bar: 50 μm. Related to Figure 4 and 7.

Figure S24. Notch is activated during repair.

(A-D) Images of Aqp2 (blue) merged with DAPI (white, left), or with B1B2 (green) and Hes1 (red, right) in UUO kidneys at D0, D6 and D14. Inserts in A and C were from different microscopic fields. Arrowheads: Hes1-expressing PC ($Aqp2^+$ $B1B2^-$), IC ($Aqp2^-$ $B1B2^+$), AP ($Aqp2^+$ $B1B2^+$) and TC4 ($Aqp2^-$ $B1B2^-$) were magnified 2.3X on the far right, with split channels. Note, no cells in the CNT/CD in C had detectable Hes1 expression. Scale bar: 50 μm. Related to Figure 7.

Figure S25. UUO progressively induces kidney fibrosis.

(A) Adult mice were subject to UUO at day 0 (d0), CldU injection at day 1 (D1), and examined 2, 6 or 14 days later (D2, D6, or D14).

(B) Mice were injected with CIdU and sacrificed one day later as non-injured control (D0).

(C-E) Correlation analyses between the percent of $Hes1^+$ cells and percent of $CIdU^+$ cells in all IC ($Aqp2^-$ $B1B2^+$) (C), PC ($Aqp2^+$ $B1B2^-$) (D), and TC4 ($Aqp2^-$ $B1B2^-$) (E). Each data point represents an individual mouse in which the correlated parameters were analyzed. A total of 8-11 mice from D0, D2, D6 and D14 post UUO (n=2-3 mice/time point) were shown.

(F-H) ImageJ-based quantification of Masson's Trichrome staining (F) and representative Masson's Trichrome staining images (G-H) showing progressive development of severe kidney fibrosis by D14 after UUO. Boxed areas in G were magnified 10X in H. Boxed areas in H were magnified 4X in Figure 7H. Scale bar: 1000 μm. n=3 mice per condition. * $p< 0.05$ vs. D0. $ $p< 0.05$ vs. D2. # $p< 0.05$ vs. D6. Related to Figures 4-8.

Movie S1. Adult AP contribute circumferentially and longitudinally to CNT/CD maintenance. Constructed 3-D structure showing XFP-labeled cells or clones of the adult *$Aqp2^{ECE/+}$ Brainbow/+* mice 300 days post1 X 2 mg Tamoxifen induction. A large YFP clone

had expanded circumferentially and longitudinally to maintain the CNT/CD. The 3-D structure was generated by confocal microscopy with 0.5 μm optical sections. Related to Figure 2

Reference

1. Gao C, Chen L, Chen E, Tsilosani A, Xia Y, Zhang W: Generation of distal renal segments involves a unique population of Aqp2+ progenitor cells *J Am Soc Nephrol*, 2021 10.1681/ASN.2021030399

2. Park J, Shrestha R, Qiu C, Kondo A, Huang S, Werth M, et al.: Single-cell transcriptomics of the mouse kidney reveals potential cellular targets of kidney disease. *Science,* 360**:** 758-763, 2018 10.1126/science.aar2131

3. Rinkevich Y, Montoro DT, Contreras-Trujillo H, Harari-Steinberg O, Newman AM, Tsai JM, et al.: In vivo clonal analysis reveals lineage-restricted progenitor characteristics in mammalian kidney development, maintenance, and regeneration. *Cell Rep,* 7**:** 1270-1283, 2014 10.1016/j.celrep.2014.04.018

4. Lazzeri E, Angelotti ML, Peired A, Conte C, Marschner JA, Maggi L, et al.: Endocycle-related tubular cell hypertrophy and progenitor proliferation recover renal function after acute kidney injury. *Nat Commun,* 9**:** 1344, 2018 10.1038/s41467-018-03753-4

5. Nandagopal N, Santat LA, Elowitz MB: Cis-activation in the Notch signaling pathway. *Elife,* 8, 2019 10.7554/eLife.37880

6. Jeong HW, Jeon US, Koo BK, Kim WY, Im SK, Shin J, et al.: Inactivation of Notch signaling in the renal collecting duct causes nephrogenic diabetes insipidus in mice. *J Clin Invest,* 119**:** 3290-3300, 2009 10.1172/JCI38416

7. Mukherjee M, deRiso J, Otterpohl K, Ratnayake I, Kota D, Ahrenkiel P, et al.: Endogenous Notch Signaling in Adult Kidneys Maintains Segment-Specific Epithelial Cell Types of the Distal Tubules and Collecting Ducts to Ensure Water Homeostasis. *J Am Soc Nephrol,* 30**:** 110-126, 2019 10.1681/ASN.2018040440

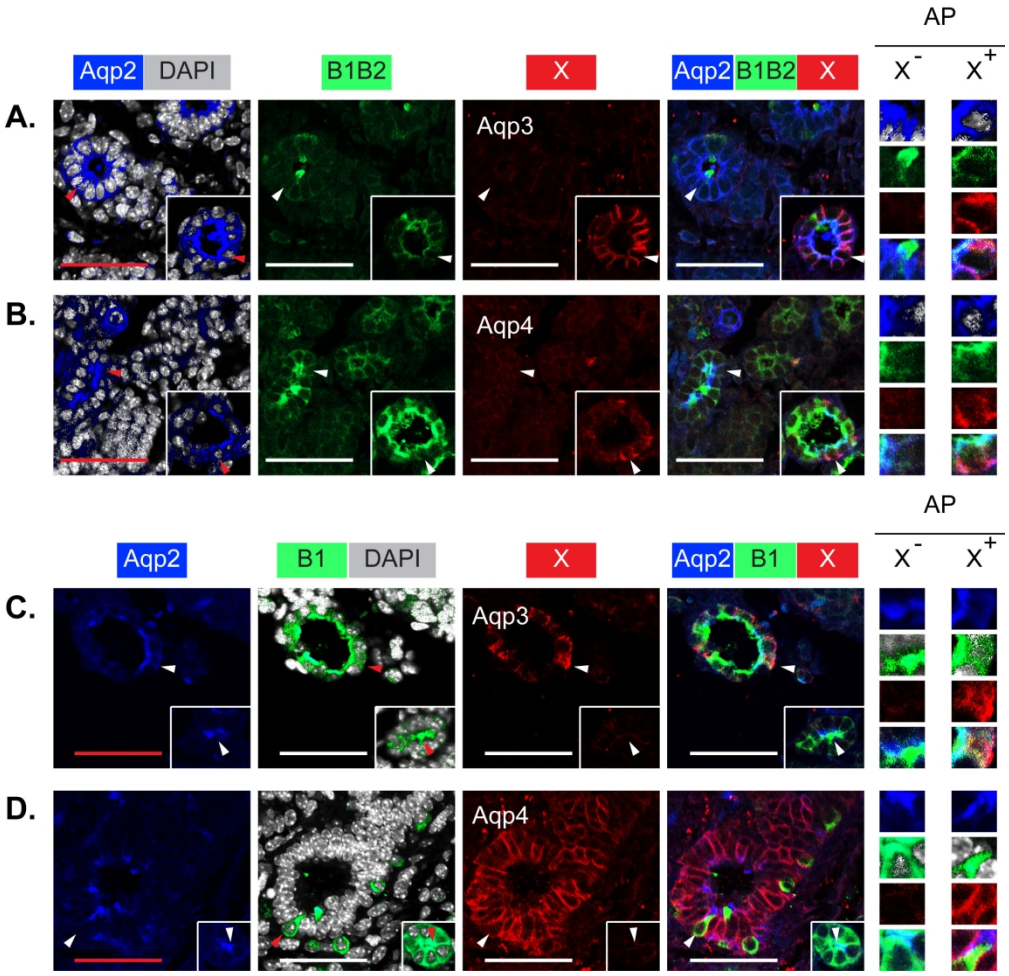

Figure S1. Aqp2+ B1B2+ and Aqp2+ B1+ cells with and without detectable expression of Aqp3 and Aqp4 exist in E15.5 kidneys.
(A-B) Images of Aqp2 (blue) merged with DAPI (white), B1B2 (green), and Aqp3 (A) or Aqp4 (B) (both in red) in E15.5 kidneys showing that some AP expressed Aqp3 and/or Aqp4 while others lacked detectable Aqp3 and/or Aqp4. Images in the inserts were from different regions of E15.5 kidneys. Arrowheads: AP were magnified 2.3X on the far right lacking or expressing Aqp3 or Aqp4.
(C-D). As in A-B, except B1B2 replaced with B1, which is merged with DAPI. Images in the inserts were from different regions of E15.5 kidneys.
Scale bar: 50 μm. Related to Figures 1 and 2.

201x195mm (300 x 300 DPI)

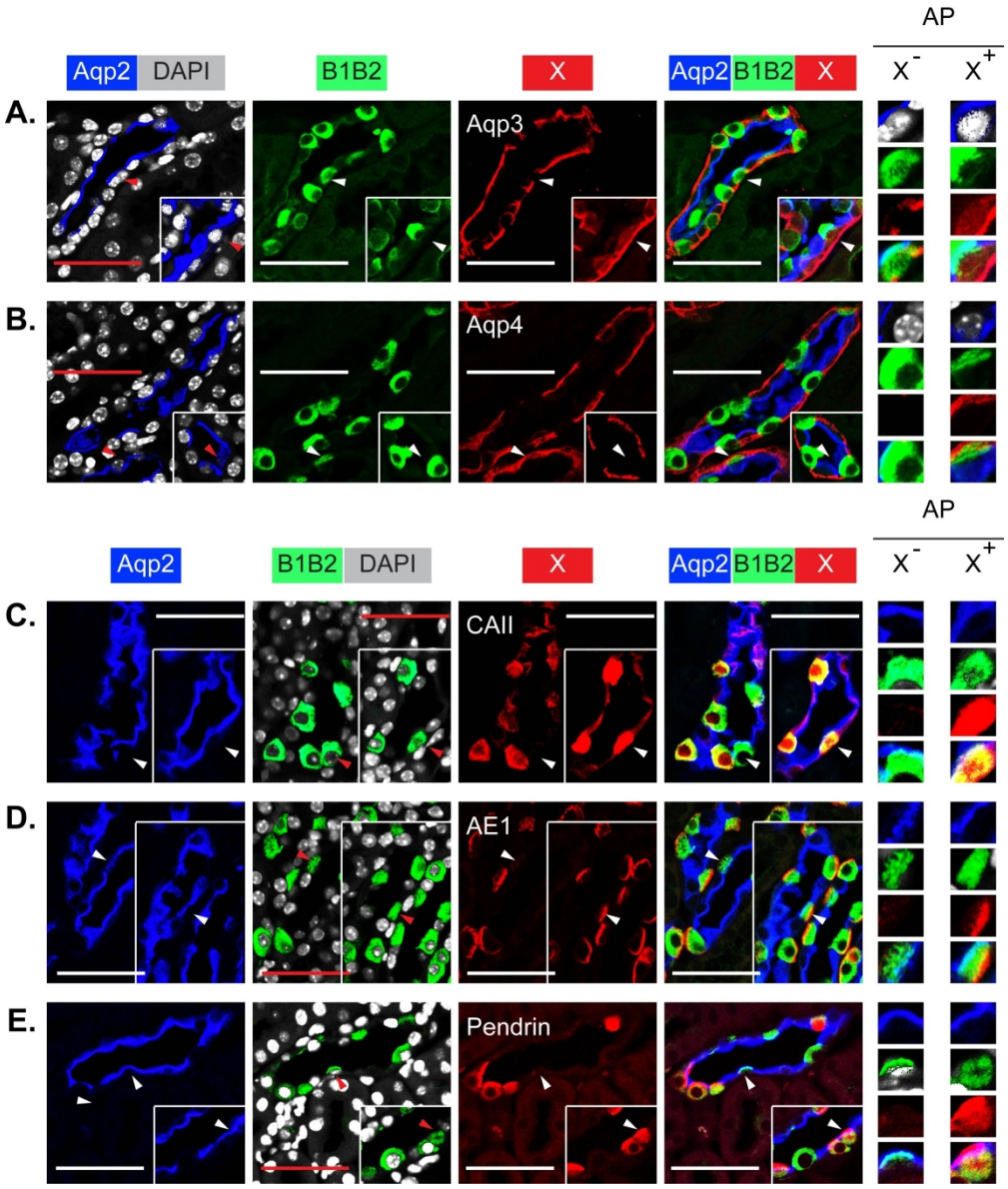

Figure S2. Aqp2+ B1B2+ cells with and without detectable expression of other PC and IC markers exist in adult WT C57Bl/6 kidneys.
(A-B) Images of Aqp2 (blue) merged with DAPI (white), B1B2 (green), and Aqp3 (A) or Aqp4 (B) (both in red) in adult WT C57Bl/6 kidneys. Images in the inserts in each panel were from different regions of the same sections. Arrowheads: AP were magnified 2.3X on the far right lacking or expressing Aqp3 or Aqp4.
(C-E) As in A, except Aqp3 replaced with X (X=CAII, AE1, or Pendrin as indicated), and B1B2 merged with DAPI. Images in the inserts in each panel were from different regions of the same sections.
Scale bar: 50 μm. Related to Figures 1 and 2.

200x236mm (300 x 300 DPI)

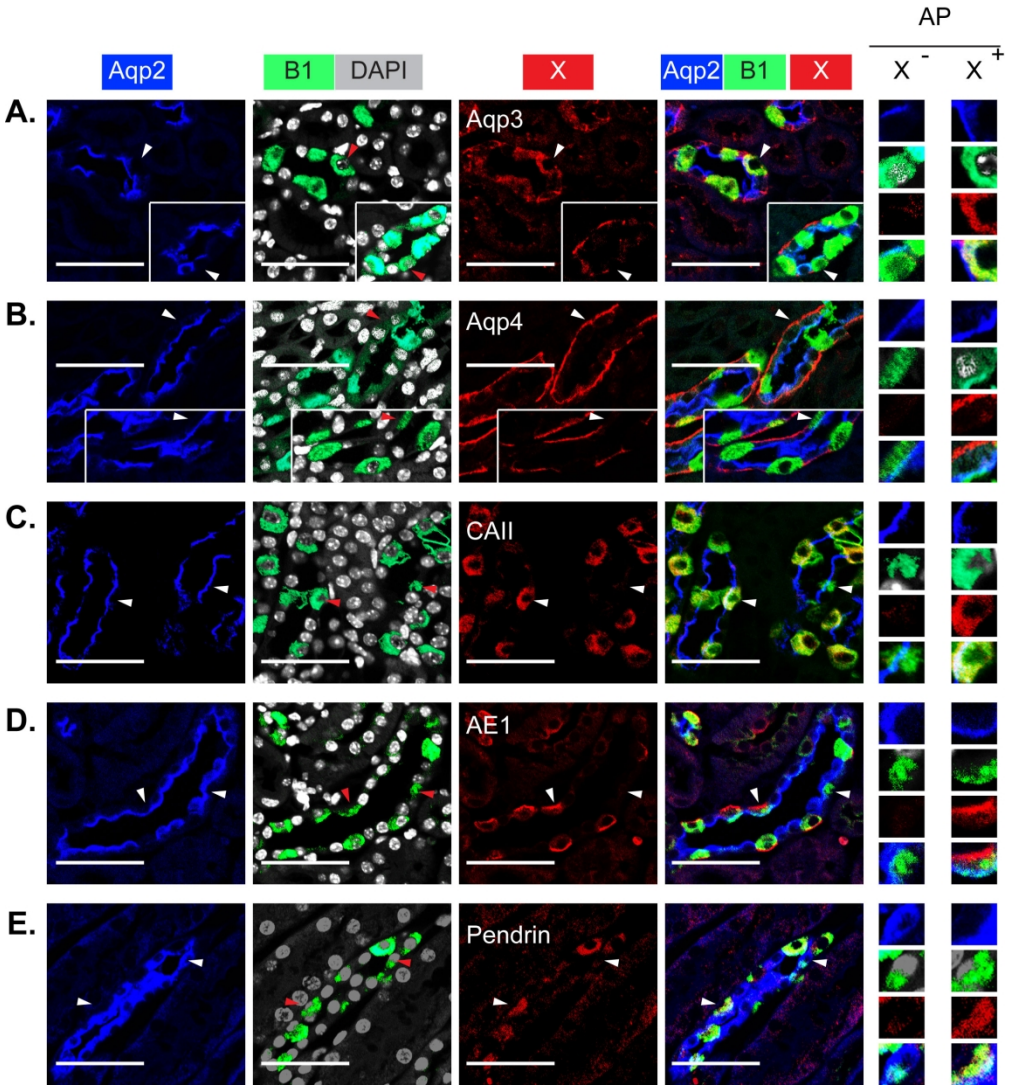

Figure S3. Aqp2+ B1+ cells with and without detectable expression of other PC and IC markers exist in adult kidneys.
(A-E) Images of Aqp2 (blue), B1 (green) merged with DAPI (white), and X (red, X=Aqp3, Aqp4, CAII, AE1, or Pendrin) in adult WT C57Bl/6 kidneys. Images in the inserts in A and B were from different regions of the same sections. In D, both rabbit B1 and AE1 primary antibodies were used sequentially in combination of monovalent Fab fragments of secondary antibodies (see Immunofluorescence studies in Methods section). Arrowheads: AP were magnified 2.3X on the far right lacking or expressing X (X= Aqp3, Aqp4, CAII, AE1, or Pendrin). Scale bar: 50 μm. Related to Figures 1 and 2.

200x216mm (300 x 300 DPI)

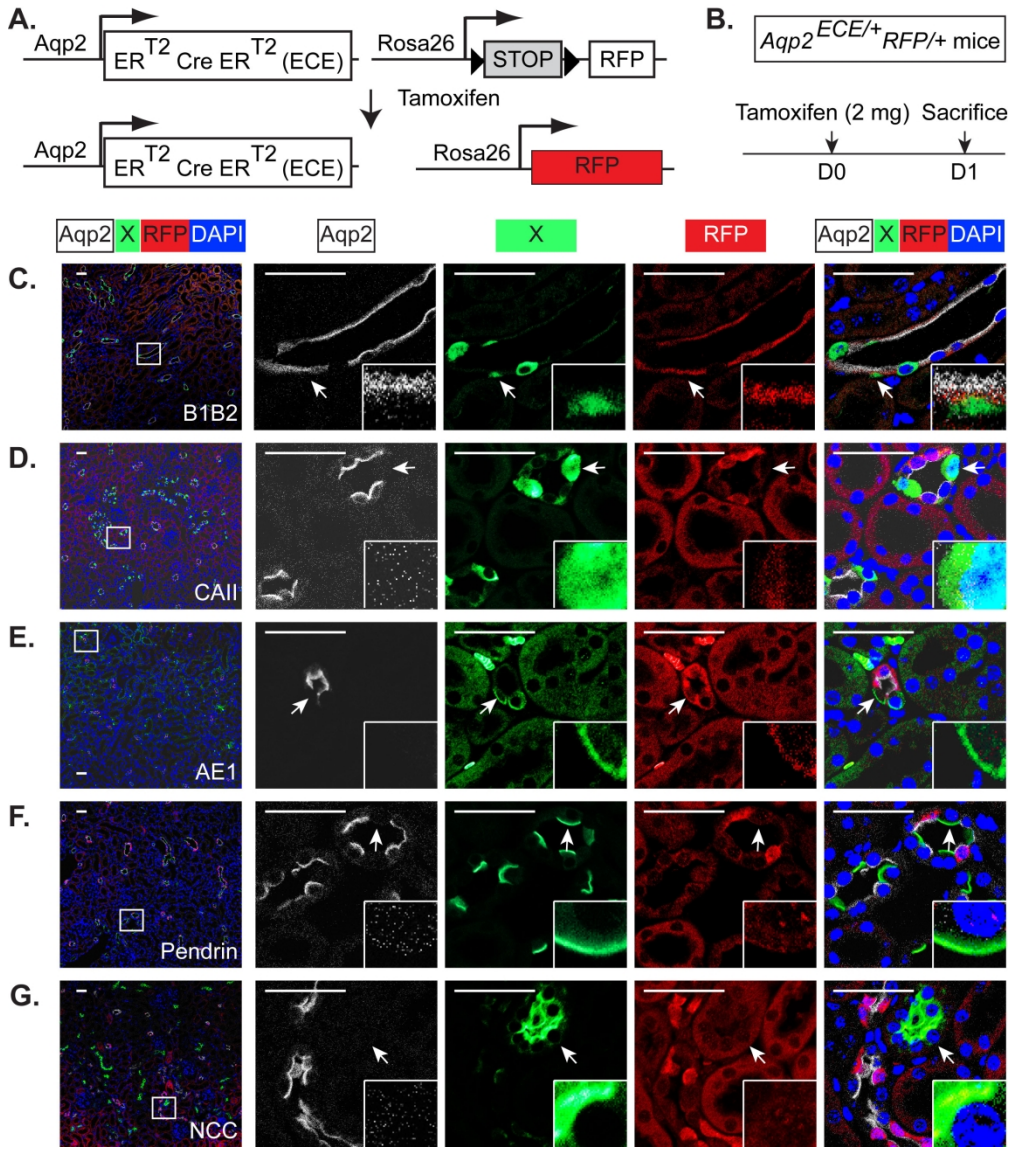

Figure S4. No converted IC and DCT2 cells in adult Aqp2ECE/+ RFP/+ mice one day after Tamoxifen induction.

(A) RFP expression in the Aqp2+ lineage after Tamoxifen induced ECE-mediated recombination in Aqp2ECE/+ RFP/+ mice. .

(B) Adult Aqp2ECE/+ RFP/+ mice were injected with 1 X 2 mg Tamoxifen at day 0 and examined at day 1 post induction (D1).

(C-G) Immunofluorescence confocal images of Aqp2 (white), RFP (red), X (green, X = V-ATPase B1B2, CAII, AE1, Pendrin, and NCC), and DAPI (blue) in adult Aqp2ECE/+ RFP/+ kidneys at day 1 post 1 X 2 mg Tamoxifen induction. Boxed areas were magnified 2X on the right, with channels split. Scale bar: 50 μm. Arrowhead: cells were magnified 4X in inserts, highlighting no conversion of Aqp2+ cells into IC or DCT2 cells during a short time period after Tamoxifen induction as detailed below.

(C) No converted Aqp2- RFP+ B1B2+ cells, despite existence of rare labeled AP (Aqp2+ B1B2+ RFP+)

(D) No converted Aqp2- RFP+ CAII+ cells.

(E) No converted Aqp2- RFP+ AE1+ cells.

(F) No converted Aqp2- RFP+ Pendrin+ cells.

(G) No converted Aqp2- RFP+ NCC+ cells.

Related to Figure 1.

218x249mm (300 x 300 DPI)

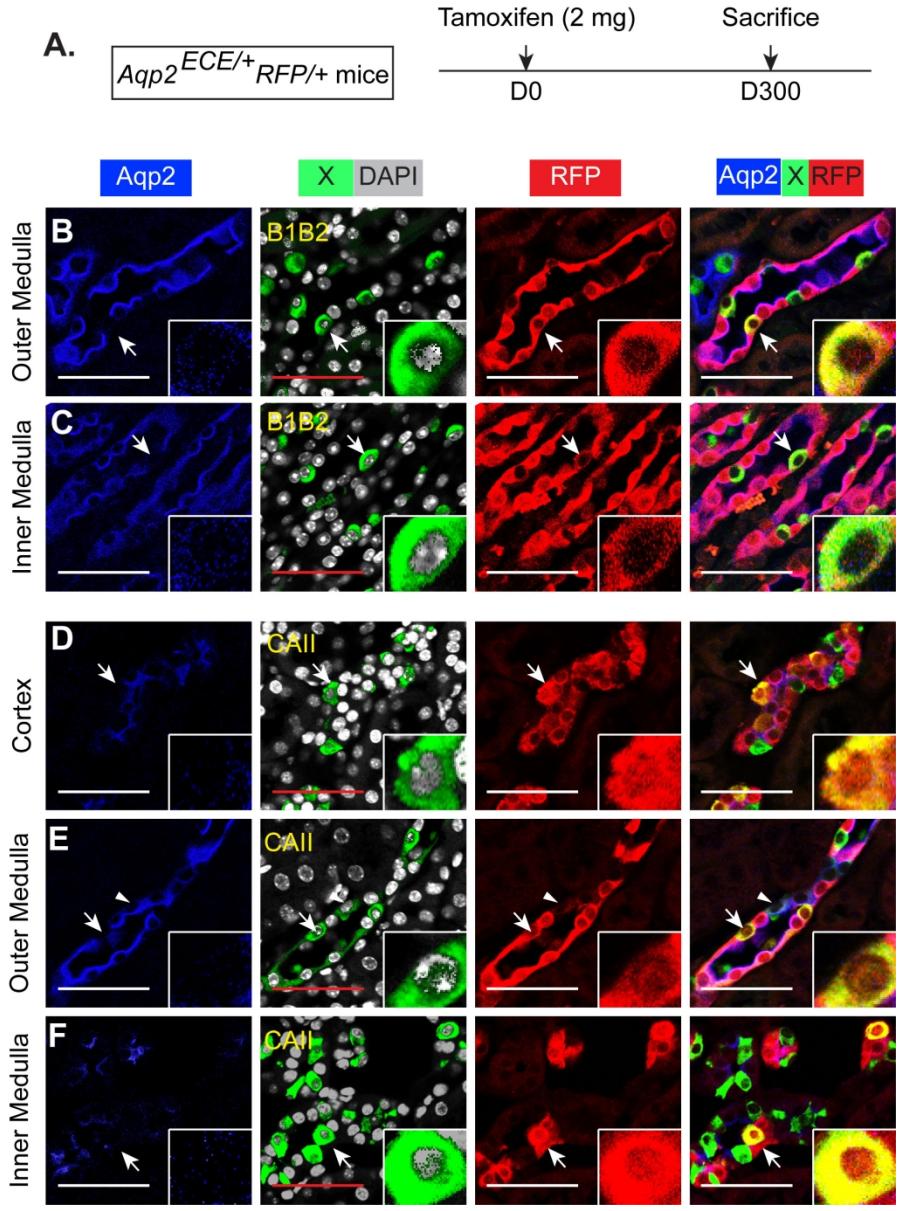

Figure S5. Converted B1B2+ and CAII+ cells in adult Aqp2ECE/+ RFP/+ mice 300 days after Tamoxifen induction.
(A) Adult Aqp2ECE/+ RFP/+ mice were injected with 1 X 2 mg Tamoxifen at day 0 and examined at day 300 post induction (D300).
(B-F) Immunofluorescence confocal images of Aqp2 (blue), X (green, X = B1B2 (B, & C) or CAII (D-F), and RFP (red)) in the regions as indicated in Aqp2ECE/+ RFP/+ kidneys at day 300. Arrows: converted cells were magnified 4X in insets and detailed below.
(B-C) Converted Aqp2- RFP+CAII+ cells.
(D-F) Converted Aqp2- RFP+CAII+ cells.
Arrowheads in E: TC1 (Aqp2+CAII+)
Scale bar: 50 μm. Related to Figures 1.

171x231mm (300 x 300 DPI)

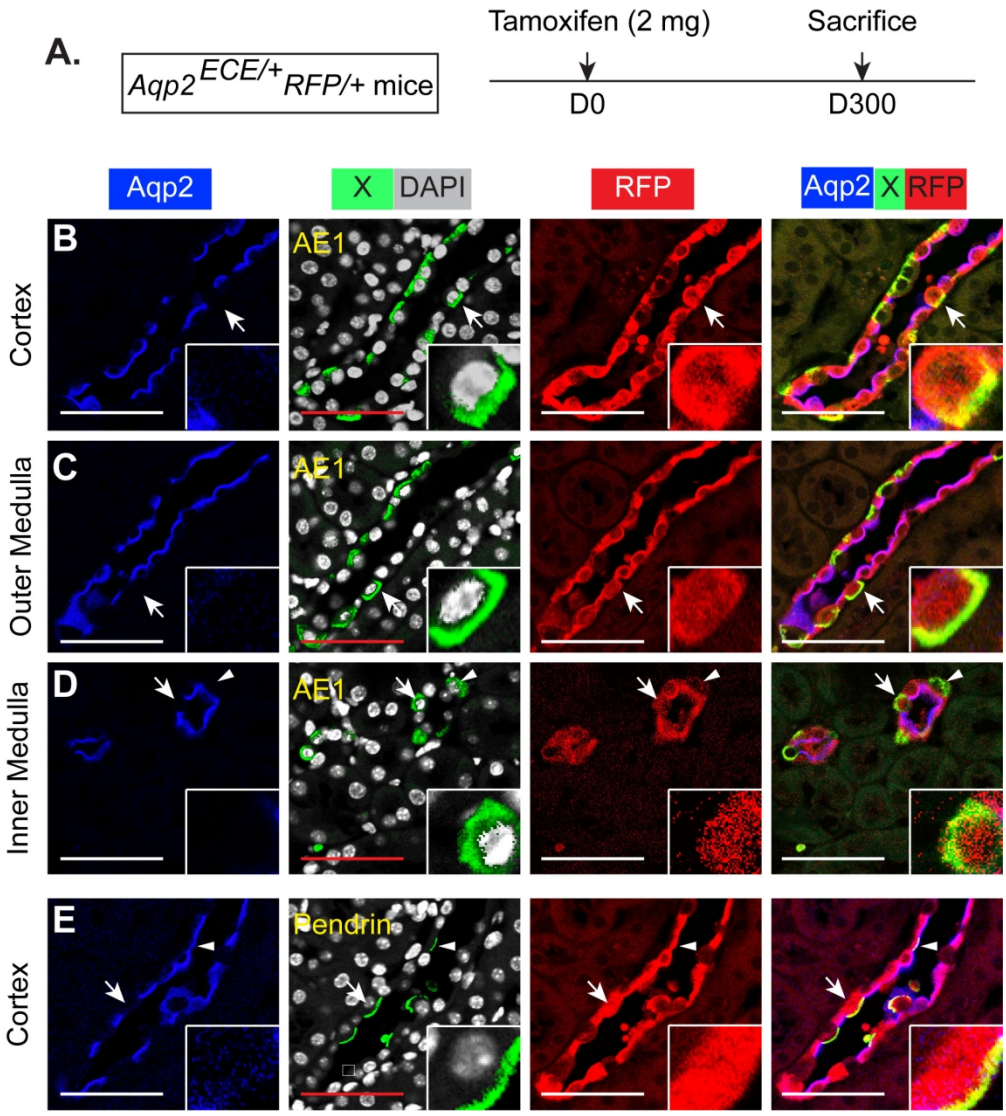

Figure S6. Converted AE1+ and Pendrin+ cells in adult Aqp2ECE/+ RFP/+ mice 300 days after Tamoxifen induction.
(A) Adult Aqp2ECE/+ RFP/+ mice were injected with 1 X 2 mg Tamoxifen at day 0 and examined at day 300 post induction (D300).
(B-E) Immunofluorescence confocal images of Aqp2 (blue), X (green, X = AE1 (B-D) or Pendrin (E), and RFP (red)) in the regions as indicated in Aqp2ECE/+ RFP/+ kidneys at day 300. Arrows: converted cells were magnified 4X in insets and detailed below.
(B-D) Converted Aqp2-RFP+AE1+ cells.
(E) Converted Aqp2-RFP+Pendrin+ cells.
Scale bar: 50 μm. Related to Figures 1.

171x189mm (300 x 300 DPI)

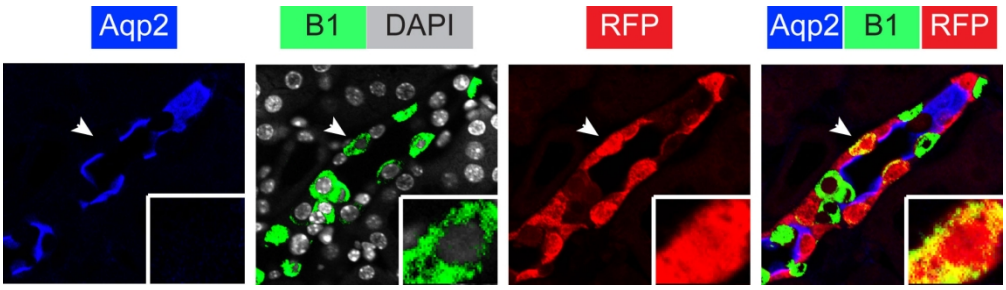

Figure S7. Converted B1+ (Aqp2-B1+RFP+) cells in adult Aqp2ECE/+ RFP/+ mice 300 days after Tamoxifen induction.
Immunofluorescence confocal images of Aqp2 (blue), B1 (green) merged with DAPI (white) and RFP (red)) in Aqp2ECE/+ RFP/+ kidneys at day 300. Arrows: a converted B1 cell (Aqp2-B1+RFP+ was magnified 4X in insets.

164x46mm (300 x 300 DPI)

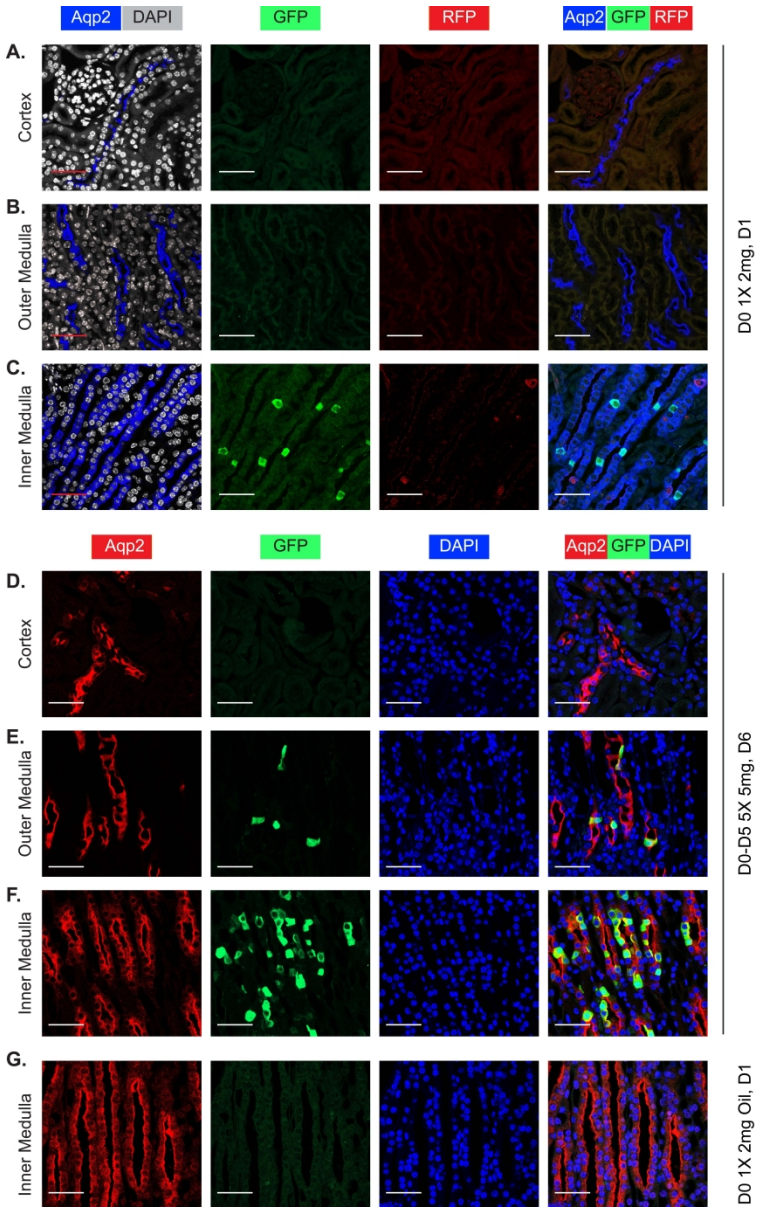

Figure S8. Optimization of Tamoxifen induction and validation of the lack of cross reactivity between the GFP and RFP antibodies in adult Aqp2ECE/+ Brainbow/+ mice.
(A-C) Adult Aqp2ECE/+ Brainbow/+ mice were induced with 1 X 2 mg Tamoxifen at D0 and analyzed at D1. Immunofluorescence confocal images of Aqp2 (blue) merged with DAPI (white), RFP (red), and GFP (green) showed individual RFP+ and GYC+ cells primarily in the inner medulla, occasionally in the outer medulla and very rarely in the cortex. The non-overlapping detection of RFP+ and GYC+ cells demonstrated the lack of cross reactivity between the GFP and RFP antibodies.
(D-F) Adult Aqp2ECE/+ Brainbow/+ mice were induced daily with 5 X 5 mg Tamoxifen at D0-D5 and analyzed at D6. Immunofluorescence confocal images of Aqp2 (red), GFP (green) and DAPI (blue) showed GYC+ "clones" with various numbers of cells primarily in the inner medulla, occasionally in the outer medulla and very rarely in the cortex.
(G) Adult Aqp2ECE/+ Brainbow/+ mice were induced with 1 X 2 mg oil at D0 and analyzed at D1. Immunofluorescence confocal images of Aqp2 (red), GFP (green) and DAPI (blue) showed no GYC+ cells in the inner medulla.

Scale bar: 50 μm. Related to Figure 2.

374x597mm (300 x 300 DPI)

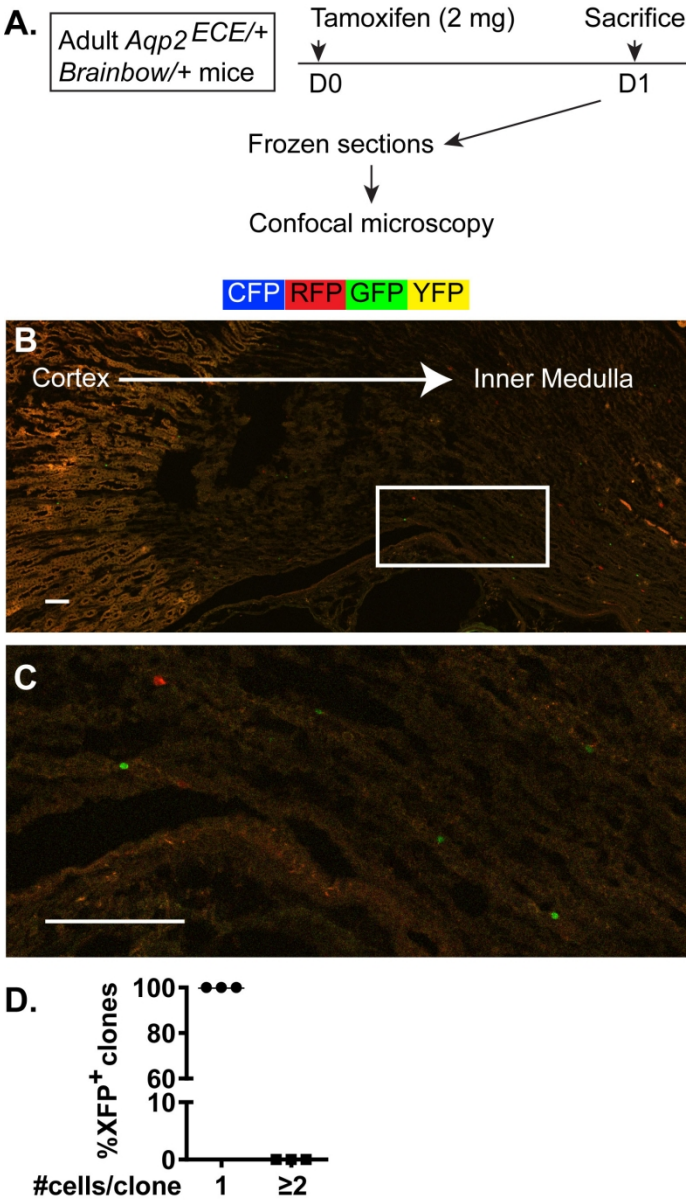

Figure S9. Individual XFP+ cells in adult Aqp2ECE/+ Brainbow/+ mice one day post 1X 2 mg Tamoxifen induction.
(A) Adult Aqp2ECE/+ Brainbow/+ mice were induced with 1 X 2 mg Tamoxifen at D0 and analyzed at D1. Frozen sections without immunofluorescence staining were subject to confocal microscopy.
(B-C) Images of frozen sections showing sparsely distributed XFP+ cells primarily in the inner medulla. Boxed area was magnified 4X in C. No antibody staining was involved.
(D) 100% XFP+ clones contained only one cell. No XFP+ clones had 2 or more XFP+ cells. A total of 1001 clones from 3 mice were examined.
Scale bar: 50 μm. Related to Figure 2.

127x223mm (300 x 300 DPI)

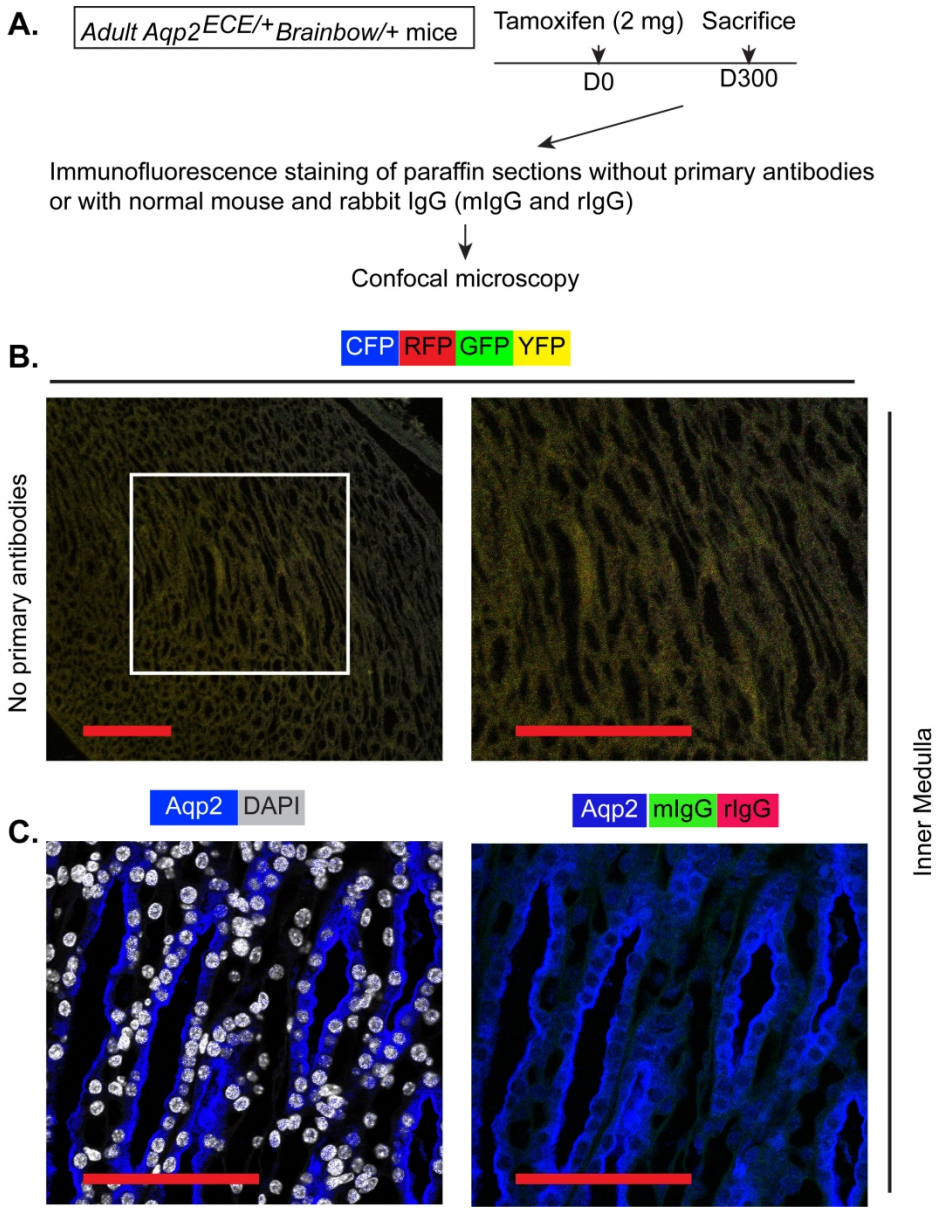

Figure S10. Validation of specific detection of XFP on paraffin sections.
(A) Adult Aqp2ECE/+ Brainbow/+ mice were induced with 1 X 2 mg Tamoxifen at D0 and analyzed at D300 for immunofluorescence staining of paraffin sections without primary antibodies or using normal mouse and rabbit IgGs.
(B) Confocal images showed no XFP+ cells when the primary antibodies were omitted. Boxed area was magnified 2X on the right.
(C) Confocal images of Aqp2 (blue) merged with DAPI (white, left), or with normal mouse IgG (mIgG, green) and normal rabbit IgG (rIgG, red) showed no XFP+ cells. In either case, no XFP+ cells were detected, demonstrating the disruption of green, red, yellow and cyan-emitting fluorophores by the immunofluorescence staining procedure and the dependence of the primary antibodies for the detection of XFP.
Scale bar: 100 μm. Related to Figure 2.

187x240mm (300 x 300 DPI)

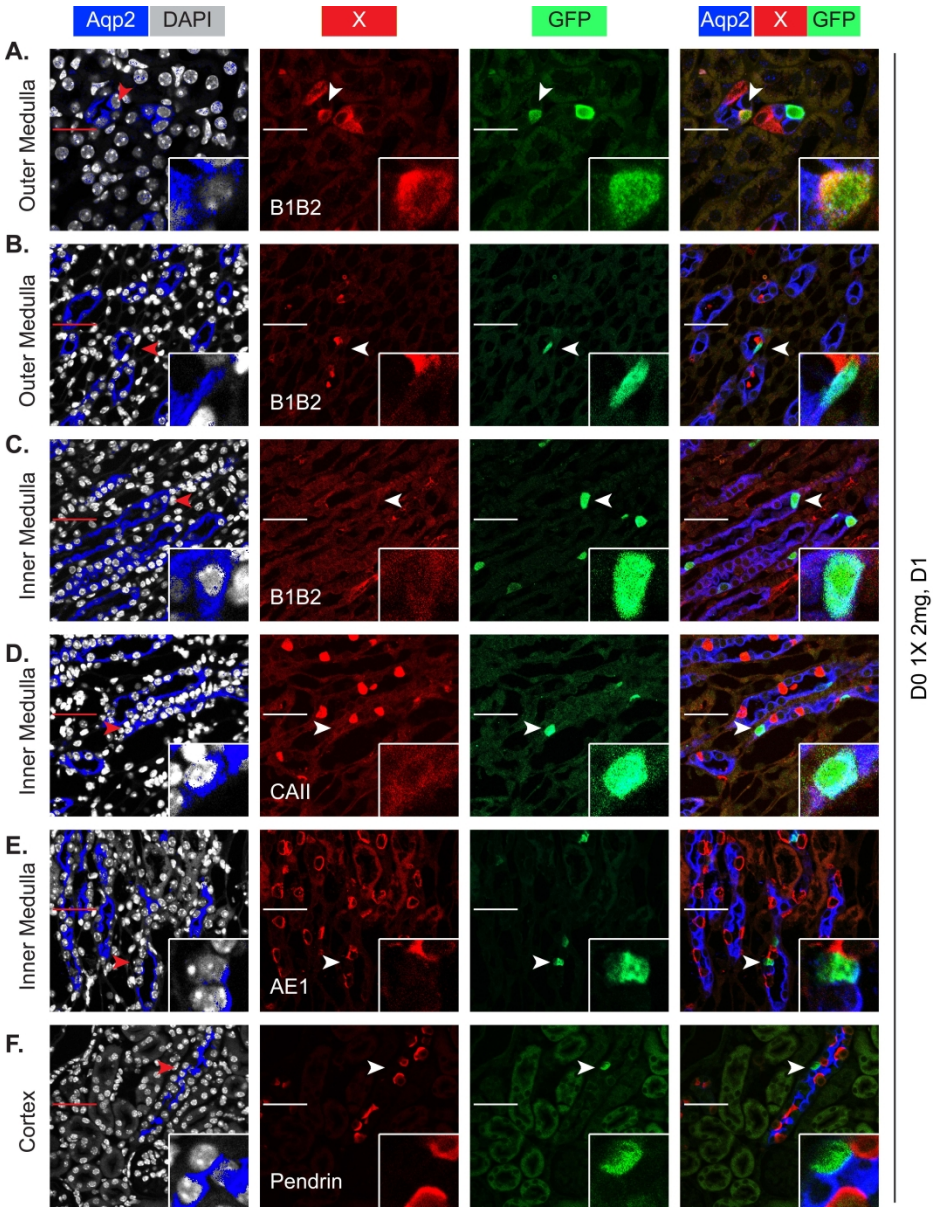

Figure S11. No converted GYC+ cells in adult Aqp2ECE/+ Brainbow/+ mice one day post induction.
(A-F) Immunofluorescence confocal images of Aqp2 (blue) merged with DAPI (white), X (X= B1B2, CAII, AE1, and Pendrin, all in red) and GYC recognized by the GFP antibody (green) showing that individual GYC+ (green) cells expressing Aqp2 with or without X throughout the Aqp2ECE/+ Brainbow/+ kidneys 1 day after 1 X 2 mg Tamoxifen injection. Arrowheads: Individual GYC+ cells magnified 4X in inserts are either AP or Aqp2+X- cells, demonstrating no Aqp2+ cells to X+ conversion as detailed below. Scale bar: 50 μm.
(A) Labeled Aqp2+ B1B2+ GYC+ cells (i.e. Labeled AP).
(B-C) No converted Aqp2- B1B2+ GYC+ cells in the outer (B) and inner medulla (C).
(D) No converted Aqp2- CAII+ GYC+ cells in the inner medulla.
(E) No converted Aqp2- AE1+ GYC+ cells in the inner medulla.
(F) A very rare GYC+ cell in the cortex that was Aqp2+ Pendrin-.
Related to Figure 2.

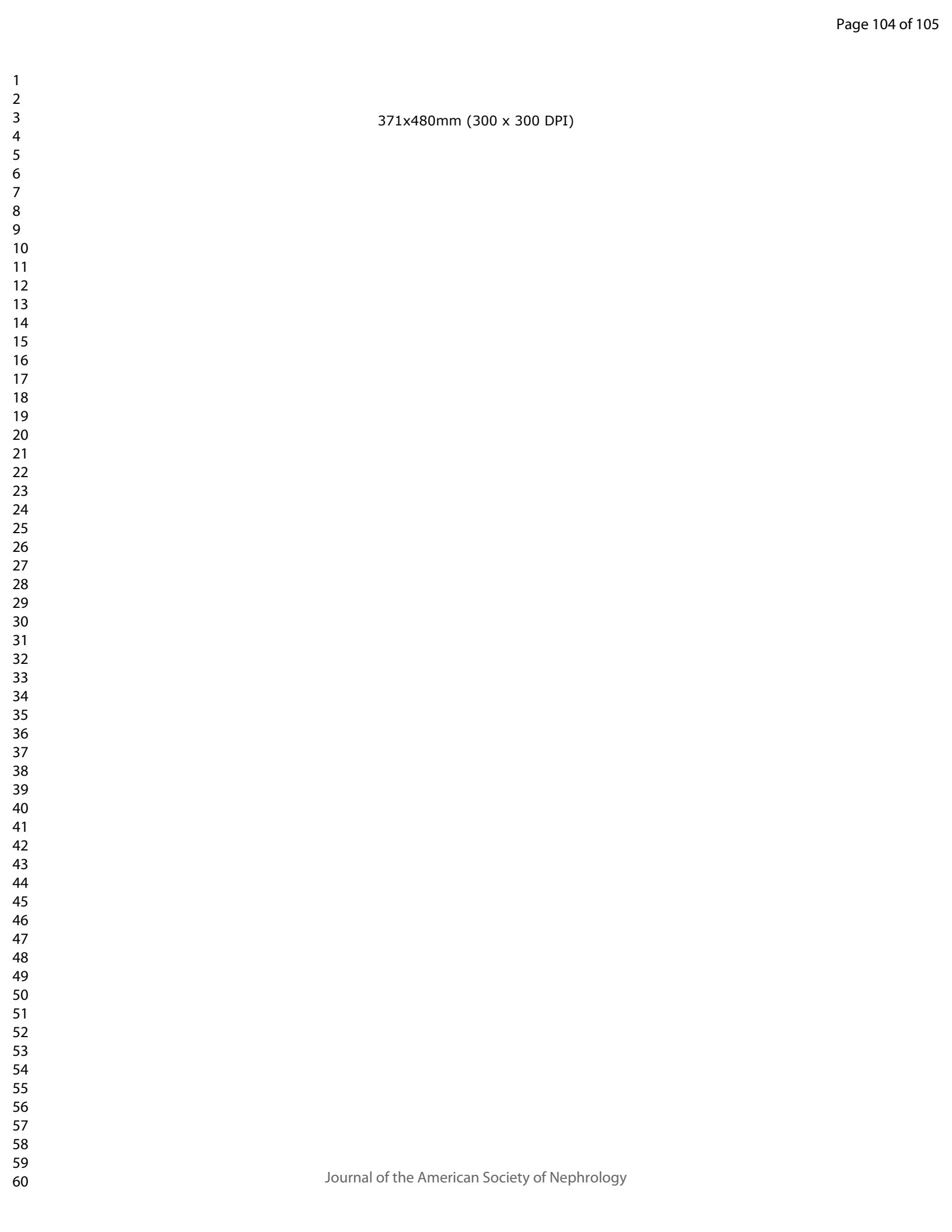
371x480mm (300 x 300 DPI)

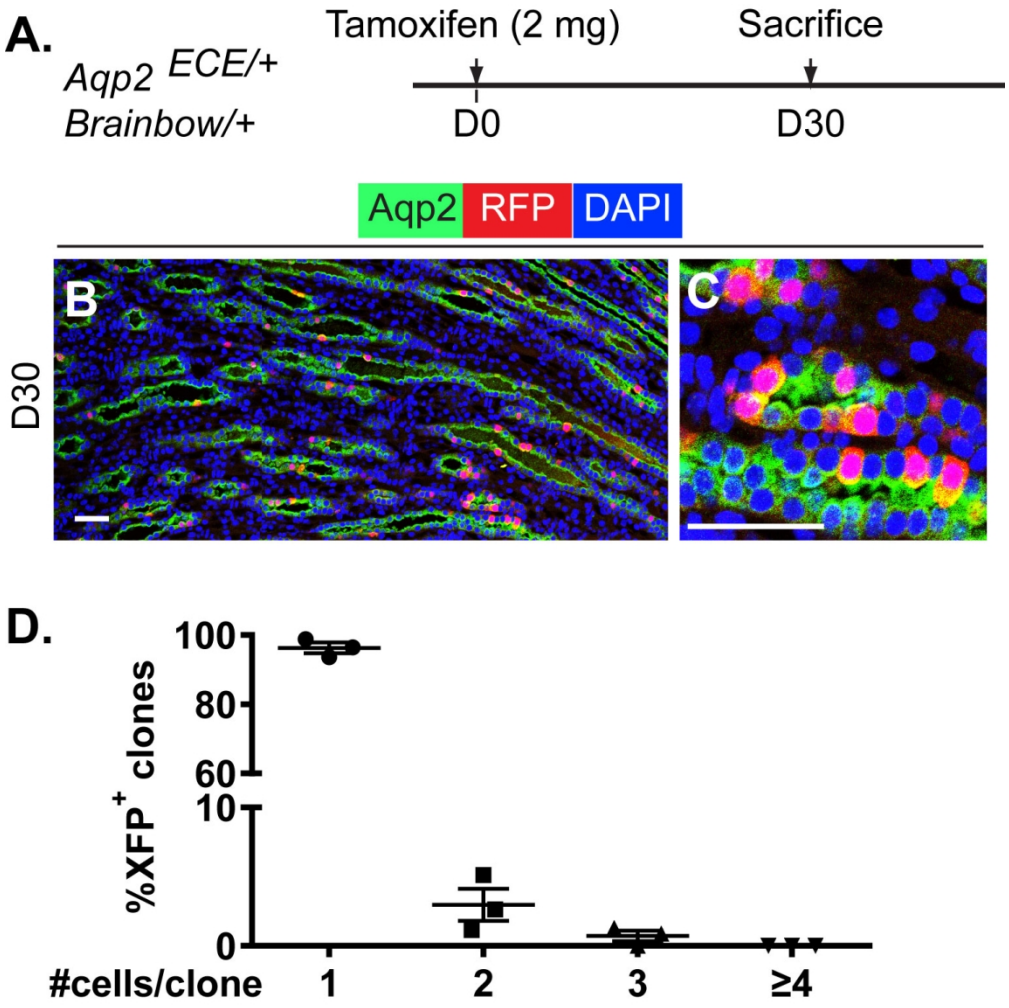

Figure S12. RFP+ clones containing 1-3 cells in adult Aqp2ECE/+ Brainbow/+ mice 30 days post induction. (A) Adult Aqp2ECE/+ Brainbow/+ mice were induced with 1 X 2 mg Tamoxifen at D0 and analyzed at D30. (B-C) Immunofluorescence confocal images of Aqp2 (green), RFP (red) and DAPI (blue) showed RFP+ "clones" with 1-3 cells in the inner medulla. Boxed area was magnified 4X in C.
(D) Percent of XFP+ clones showing that 99.4% XFP+ clones had 1-2 cells. The remaining 0.6% clones had 3 cells XFP+ clones. No XFP+ clones had 4 or more XFP+ cells. A total of 1203 clones from 3 mice were examined. Scale bar: 50 μm. Related to Figure 2.

129x130mm (300 x 300 DPI)

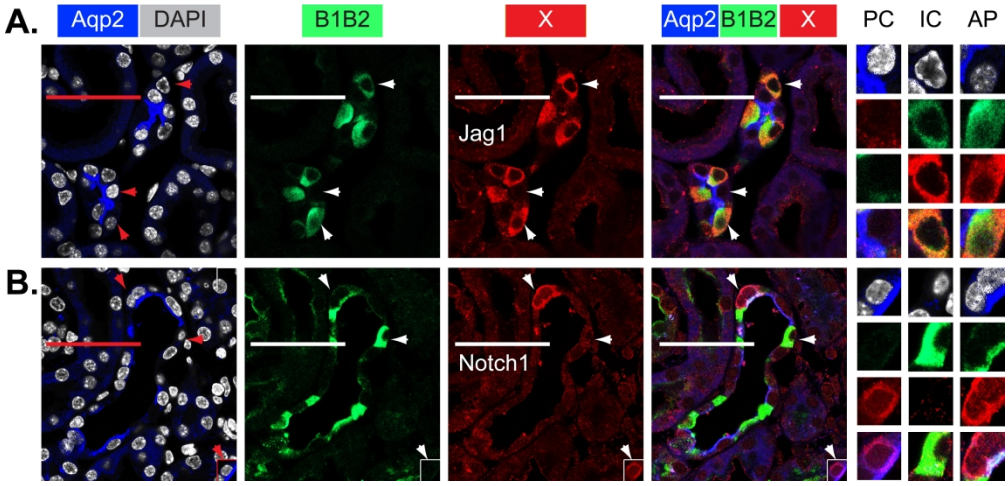

Figure S13. Adult AP express Jag1 and Notch1.
(A-B) Images of Aqp2 (blue) merged with DAPI (white), B1B2 (green), and X (X=Jag1 or Notch, both in red) in adult WT C57Bl/6 kidneys showing that AP express Jag1 and Notch1. Notch1 and Jag1 were also expressed in PC and IC, respectively. The 4th row of small enlarged panels at the right of each lettered subpanel presents the Aqp2/B1B2/X merged image. Scale bar: 50 μm. Related to Figures 1 and 2.

372x177mm (300 x 300 DPI)

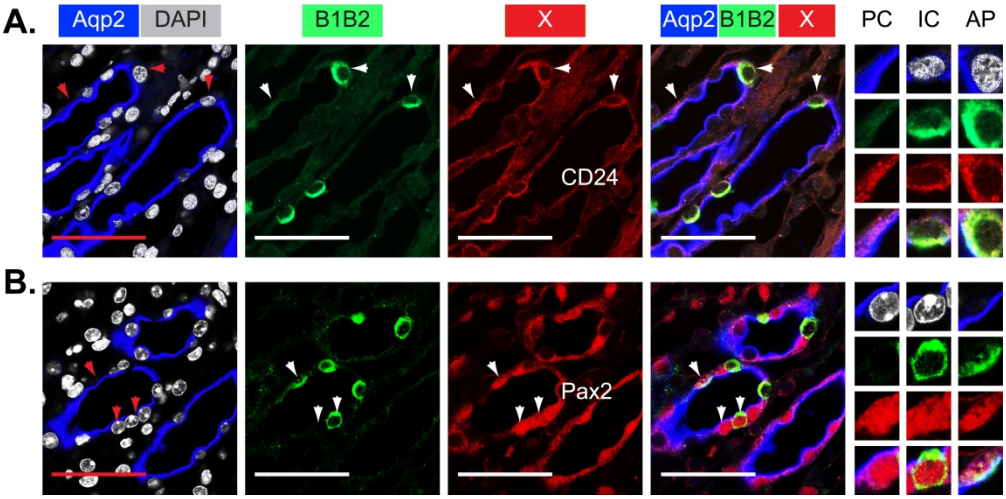

Figure S14. Adult AP express CD24 and Pax2.
(A-B) Images of Aqp2 (blue) merged with DAPI (white), B1B2 (green), and X (X=CD24, or Pax2, both in red) in adult WT C57Bl/6 kidneys showing that AP, like PC and IC, express CD24 and Pax2,. The 4th row of small enlarged panels at the right of each lettered subpanel presents the Aqp2/B1B2/X merged image. Scale bar: 50 μm. Related to Figures 1 and 2.

373x183mm (300 x 300 DPI)

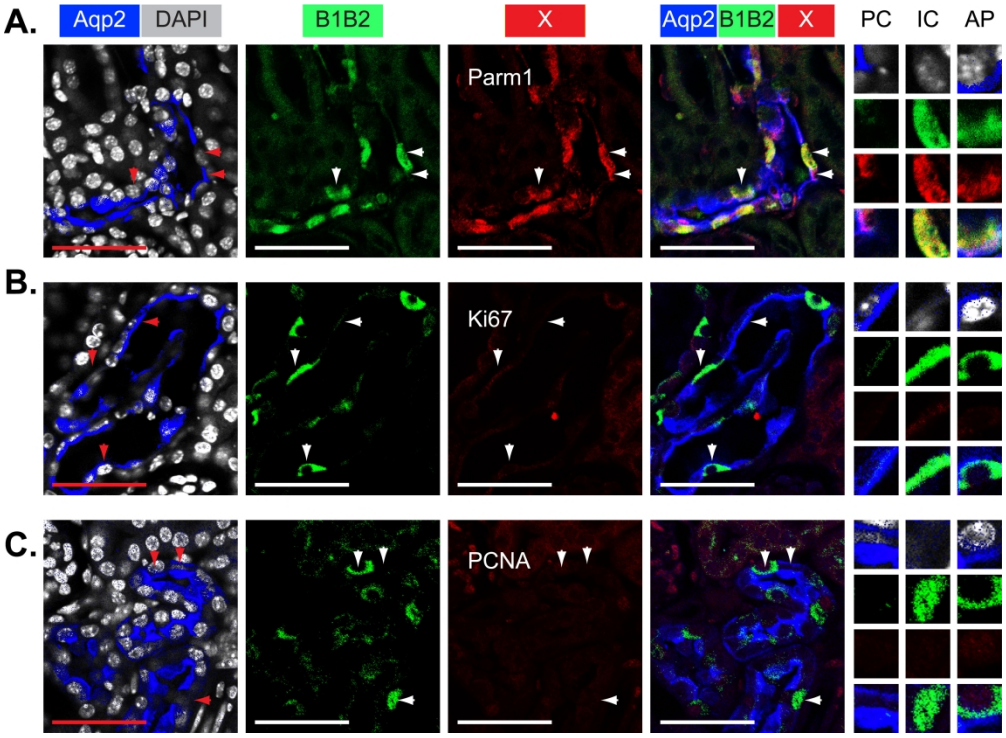

Fig. S15. Adult AP express Parm1, but not Ki67 and PCNA.
(A-C) Images of Aqp2 (blue) merged with DAPI (white), B1B2 (green), and X (X=Parm1, Ki67 or PCNA, all in red) in adult WT C57Bl/6 kidneys showing that AP, like PC and IC, express Parm1, but neither Ki67 nor PCNA. The 4th row of small enlarged panels at the right of each lettered subpanel presents the Aqp2/B1B2/X merged image. Scale bar: 50 μm. Related to Figures 1 and 2.

373x272mm (300 x 300 DPI)

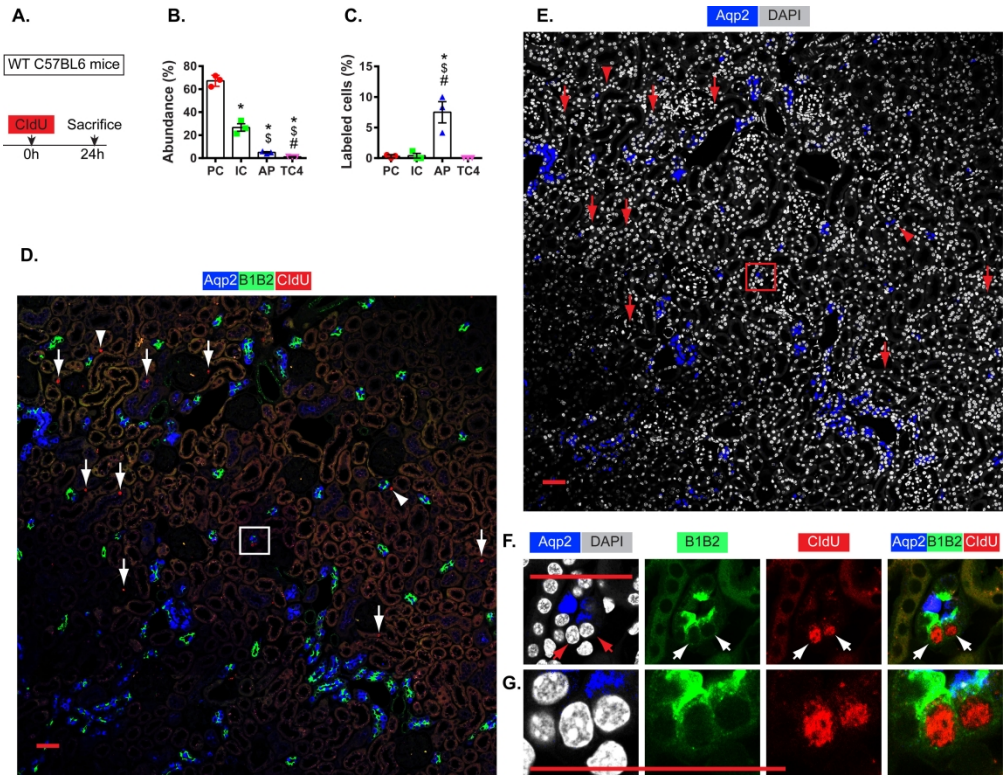

Figure S16. Adult AP occasionally and selectively divide during renal maintenance.
(A) Adult WT mice were injected with CldU (50 mg/kg BW) at 0h without UUO. Mice were analyzed at 24h.
(B) Percent of various CNT/CD cells: PC (Aqp2+ B1B2-), IC (Aqp2- B1B2+), AP (Aqp2+ B1B2+), and TC4 (Aqp2- B1B2-) throughout the kidney. A total of 5520 cells from 3 mice were counted and classified into PC, IC, AP or TC4. Error bars represent ± SEM.
(C) Percent of CIdU-labeled various CNT/CD cells throughout the kidney. A total of 5520 cells from 3 mice were counted and classified into PC, IC, AP or TC4. For each cell type, cells were then scored as CIdU+ and CIdU-, respectively (see text for details). Error bars represent ± SEM.
(D-E) Matched immunofluorescence confocal images of Aqp2 (blue) merged with B1B2 (green) and CIdU (red, D), or with DAPI (white, E) in the chased kidney. Boxed area in D was matched with boxed area in E, and magnified 4.5X in F, highlighting a 2-cell CIdU+ clone containing an AP (Aqp2+ B1B2+) and IC (Aqp2- B1B2+), with separated channels. No other CIdU+ CNT/CD cells were found throughout the image (D-E). Arrows and arrowheads in D & E: All other CIdU+ cells in Aqp2- tubules and interstitial structures, respectively. Arrows in F: The 2-cell CIdU+ clone magnified 2,5X in G. Scale bar: 50 μm.

345x265mm (300 x 300 DPI)

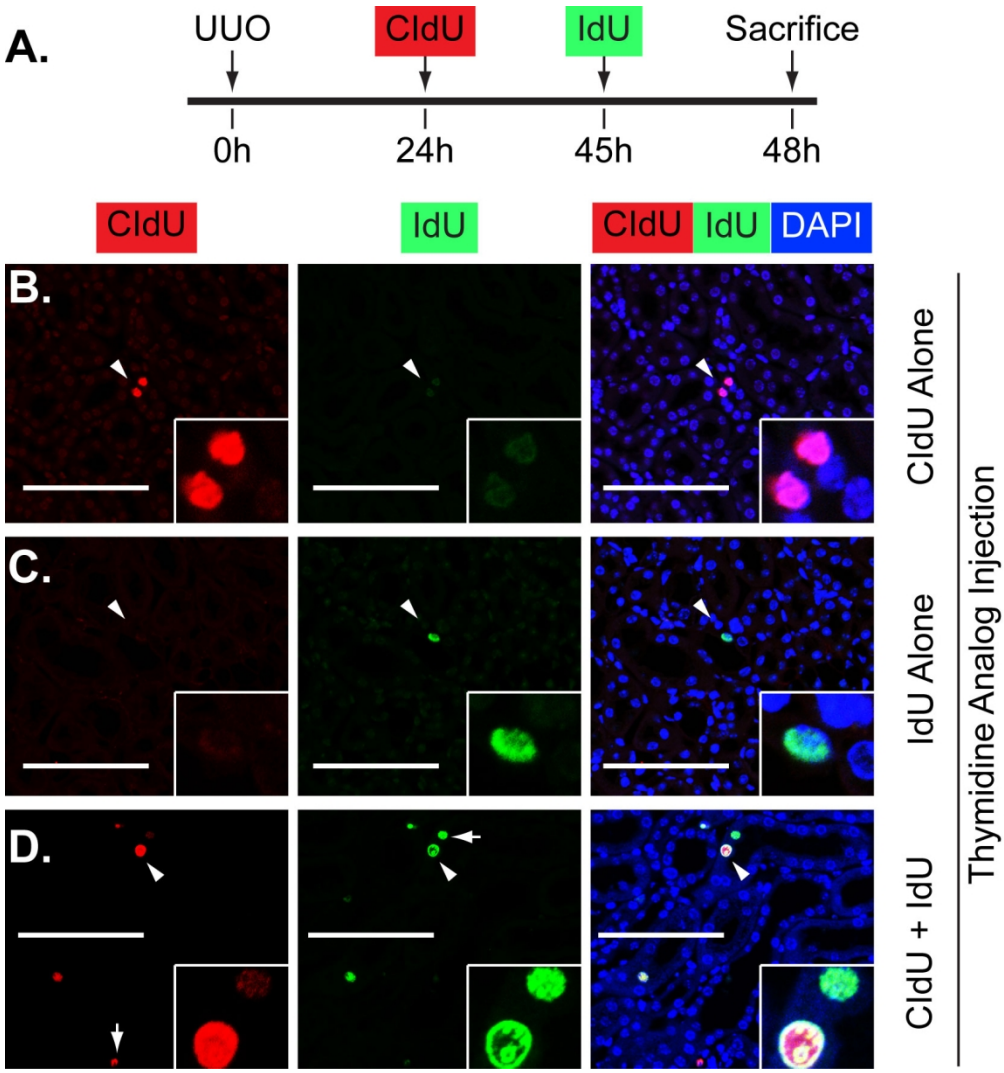

Figure S17. Validation of specific detection of CIdU and IdU.
(A) Adult mice were subject to UUO at 0h, followed by injection of CldU, IdU or in combination (50 mg/kg BW each), respectively, at 24h post UUO. For combinational injection, IdU was injected at 45h post UUO. Mice were analyzed at 48h.
(B-D) Images showing CIdU (red) and IdU (green) labeling in the kidneys. When either CldU (B) or IdU (C) was administrated alone no cross-reactivity was detected, and when both CldU and IdU (D) were sequentially injected, cells labeled by CIdU, IdU or both were found. Scale bar: 50 μm. Arrowheads: Cells were magnified 4X in inserts. Arrow in D: CIdU+ or IdU+ cells. Related to Figures 3-5, and 7.

140x149mm (300 x 300 DPI)

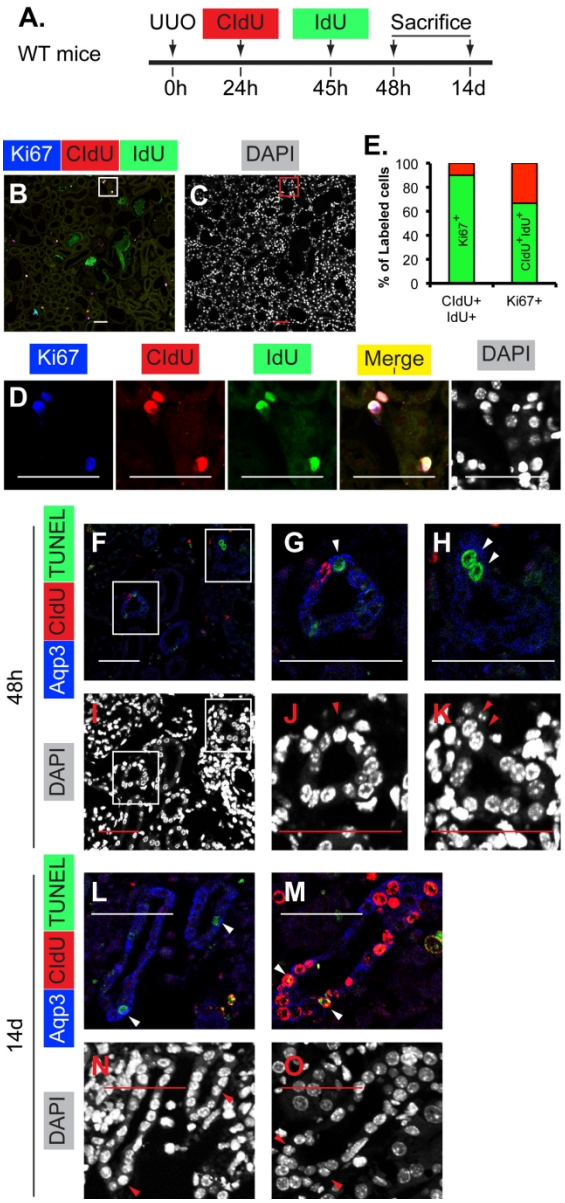

Figure S18. UUO-induced injury repair involves specific CNT/CD cells as the first responders.
(A) Adult mice were subject to UUO, and injected with CldU 24h after injury and IdU at 45h after injury. Mice were sacrificed at 48h or day 14 (14d) post-UUO.
(B-D) Immunofluorescence confocal images of Ki67 (blue), CIdU (red), IdU (green) and DAPI (white) in UUO kidneys at 48h. The boxed area in B was matched with boxed area in C and magnified 6X in D with separated channels. The 4th panel in D presents the Ki67/CIdU/IdU merged image.
(E) Percent of Ki67+ cells in CIdU+IdU+ cells (left, green) and CIdU+IdU+ cells in Ki67+ cells (right, green) in UUO kidneys at 48h. The red portions of bars show percent of Ki67- cells in CIdU+IdU+ cells (left), and percent of CIdU-, IdU-, or CIdU-IdU- cells in Ki67+ cells (right) in UUO kidneys at 48h. From 3 mice, 500 CIdU+IdU+ and 801 Ki67+ cells were counted.
(F-K) Immunofluorescence confocal images of Aqp3 (blue), CIdU (red), TUNEL (green) and DAPI (white) in UUO kidneys at 48h. Boxed regions in F were matched with boxed areas in I, and magnified 3X to highlight that injured CNT/CDs either containing apoptotic cells had (G and J) or lacked (H and K) CIdU+ cells. Arrowheads: apoptotic cells.

(L-O) Immunofluorescence confocal images of Aqp3 (blue), CIdU (red), TUNEL (green) and DAPI (white) in UUO kidneys at 14d. Injured CNT/CDs containing apoptotic cells either lacked (L and N) or had (M and O) CIdU+ cells, respectively. Arrowheads: apoptotic cells.
Scale bar: 50 μm. Related to Figure 3-4.

131x278mm (300 x 300 DPI)

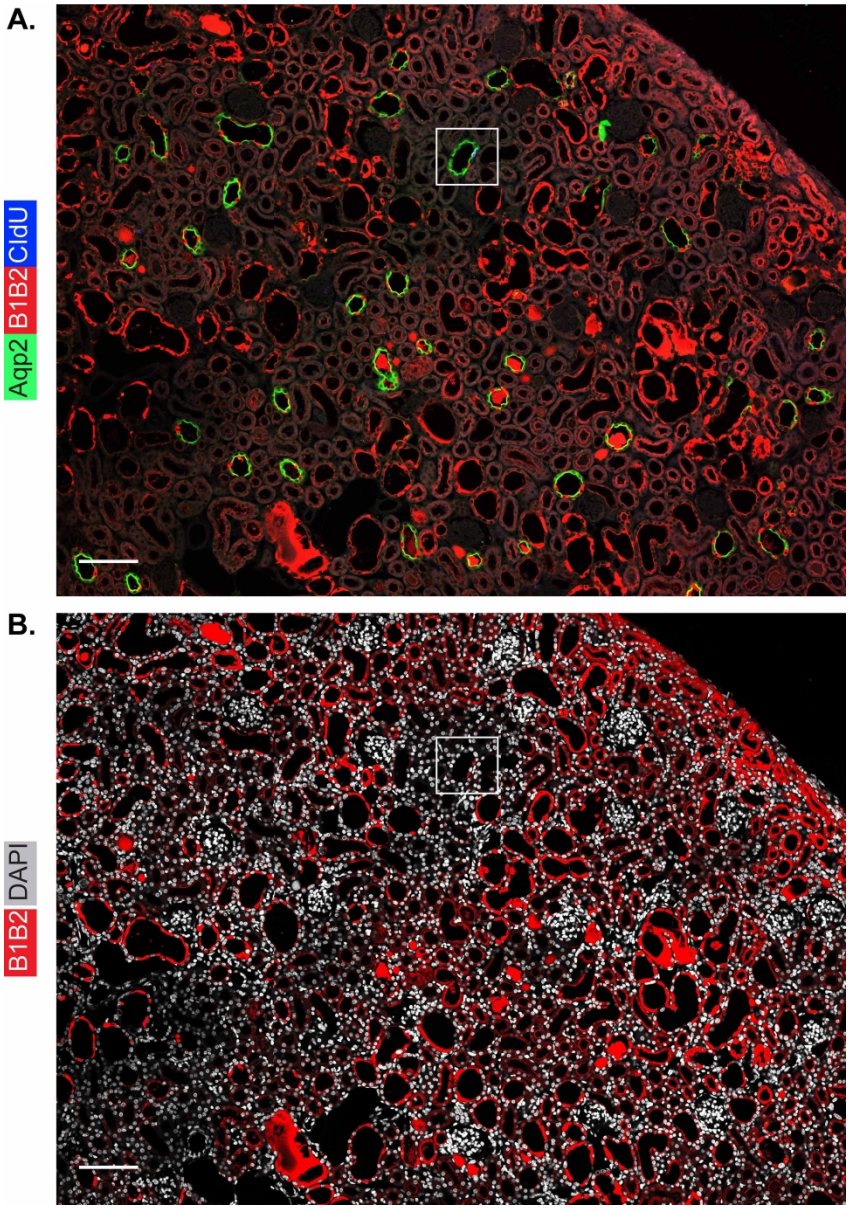

Figure S19. Adult AP selectively proliferate in response to UUO-induced injury at D2.
(A-B) Adult WT mice were subject to UUO at day 0 (d0), CIdU injection at day 1 (D1), and examined at 2 days later (D2). Matched images of Aqp2 (green), B1B2 (red) merged with DAPI (white), and CIdU (blue) showing two adjacent labeled AP (Aqp2+ B1B2+ CIdU+) in the boxed region as the sole CIdU+ CNT/CD cells in the whole area examined, demonstrating the selective proliferation of AP in UUO kidneys at D2. Boxed areas in A and B were matched and magnified 8X in Figure 4F. No other CIdU+ CNT/CD cells were found throughout the images in A and B.

273x390mm (300 x 300 DPI)

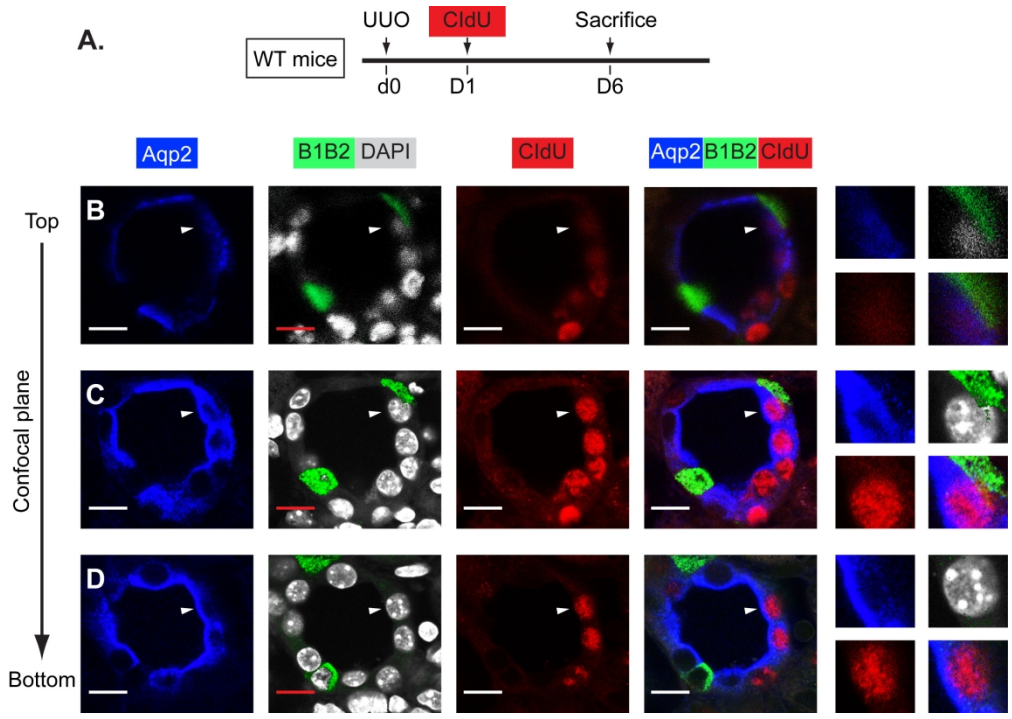

Figure S20. Adult AP exist in the expanded CIdU+ clones.
(A) Adult mice were subject to UUO at d0, followed by CIdU injection at D1, and examined at D6. (B-D) Images of three confocal planes from the top to the bottom showing the same CIdU-labeled CNT/CD in a UUO kidney, with Aqp2 (blue), B1B2 (green) merged with DAPI (white), and CIdU (red). Arrowheads: AP (B & C) and PC (D) were magnified 2.3X in far right, highlighting the lack of AP detection in the CIdU+ clone (D) because AP resides in different confocal planes (B & C). Scale bar: 50μm. Related to Figure 4.

230x162mm (300 x 300 DPI)

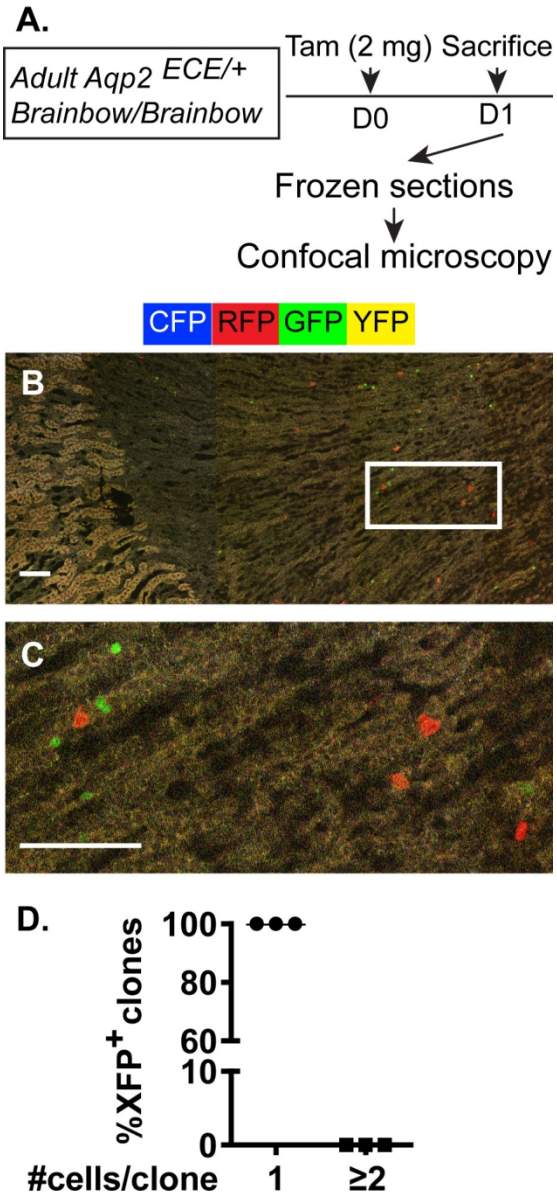

Figure S21. Sparsely distributed individual XFP+ cells were induced in the adult Aqp2ECE/+ Brainbow/Brainbow mice.
(A) Adult Aqp2ECE/+ Brainbow/Brainbow mice were induced with 1 X 2 mg Tamoxifen at D0 and sacrificed 24hrs later (D1) without UUO for confocal microscopy of frozen sections.
(B-C) Images of frozen sections of adult Aqp2ECE/+ Brainbow/Brainbow mice at D1 showing sparsely distributed individual XFP-labeled cells (X=G, Y, C and R). Boxed area in B is magnified 4X to highlight individual XFP+ cells in the inner medulla (C). No antibody staining was involved. n=3 mice.
(D) Percent of XFP+ clones containing 1, 2 or more continuous XFP+ cells of the same color without interruption by an unlabeled cell or by a cell labeled by a different color at D1. Clones of 2 or more XFP+ cells were not found. A total of 1105 clones from 3 mice were analyzed.
Scale bar: 50 μm. Related to Figure 6.

79x173mm (300 x 300 DPI)

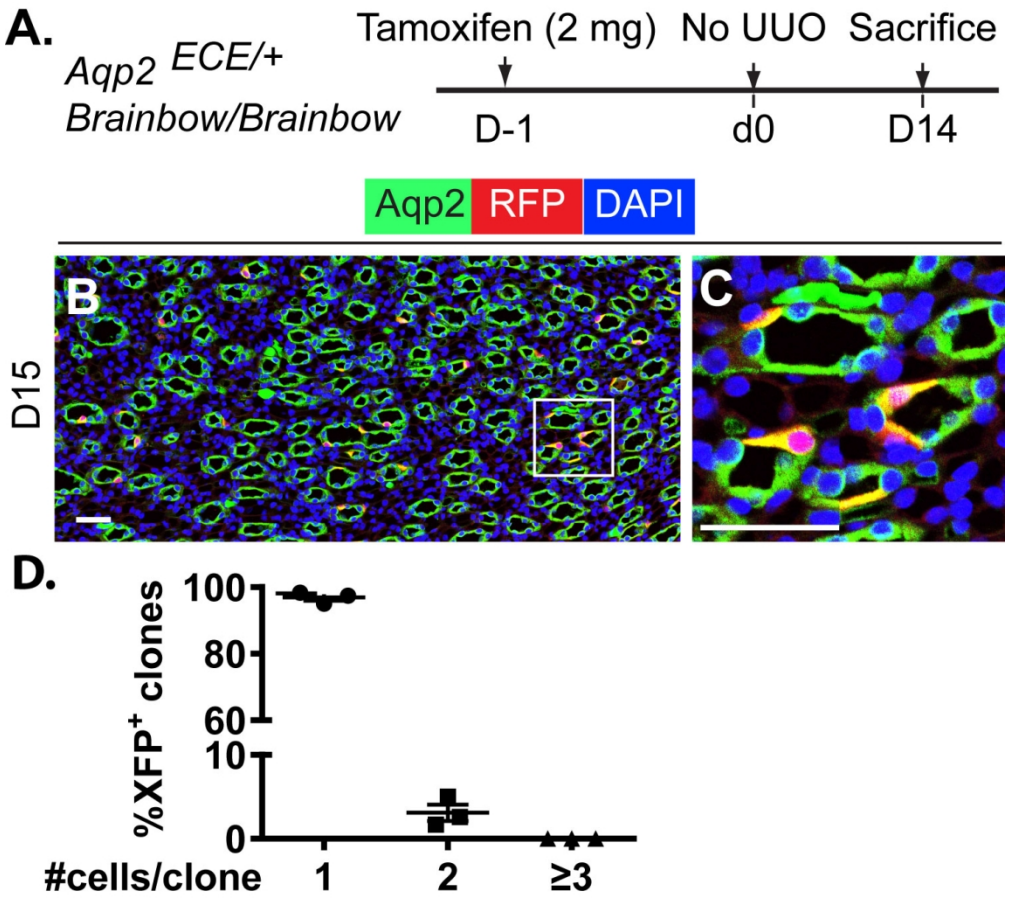

Figure S22. RFP+ clones with 1-2 cells were induced in the adult Aqp2ECE/+ Brainbow/Brainbow mice at D14.
(A) Adult Aqp2ECE/+ Brainbow/Brainbow mice were induced with 1 X 2 mg Tamoxifen at D-1, without UUO at d0, and sacrificed at D14 as non-injured control. The time points were matched with the UUO mice at D14 shown in Figure 6.
(B-C) Immunofluorescence confocal images of Aqp2 (green), RFP (red) and DAPI (blue) showed RFP+ "clones" with 1-2 cells in the inner medulla. Boxed area was magnified 4X in C.
(D) Percent of XFP+ clones showing that 100% XFP+ clones had 1-2 cells. Clones of 3 or more XFP+ cells were not observed. A total of 605 clones from 3 mice were analyzed.
Scale bar: 50 μm. Related to Figure 6.

127x114mm (300 x 300 DPI)

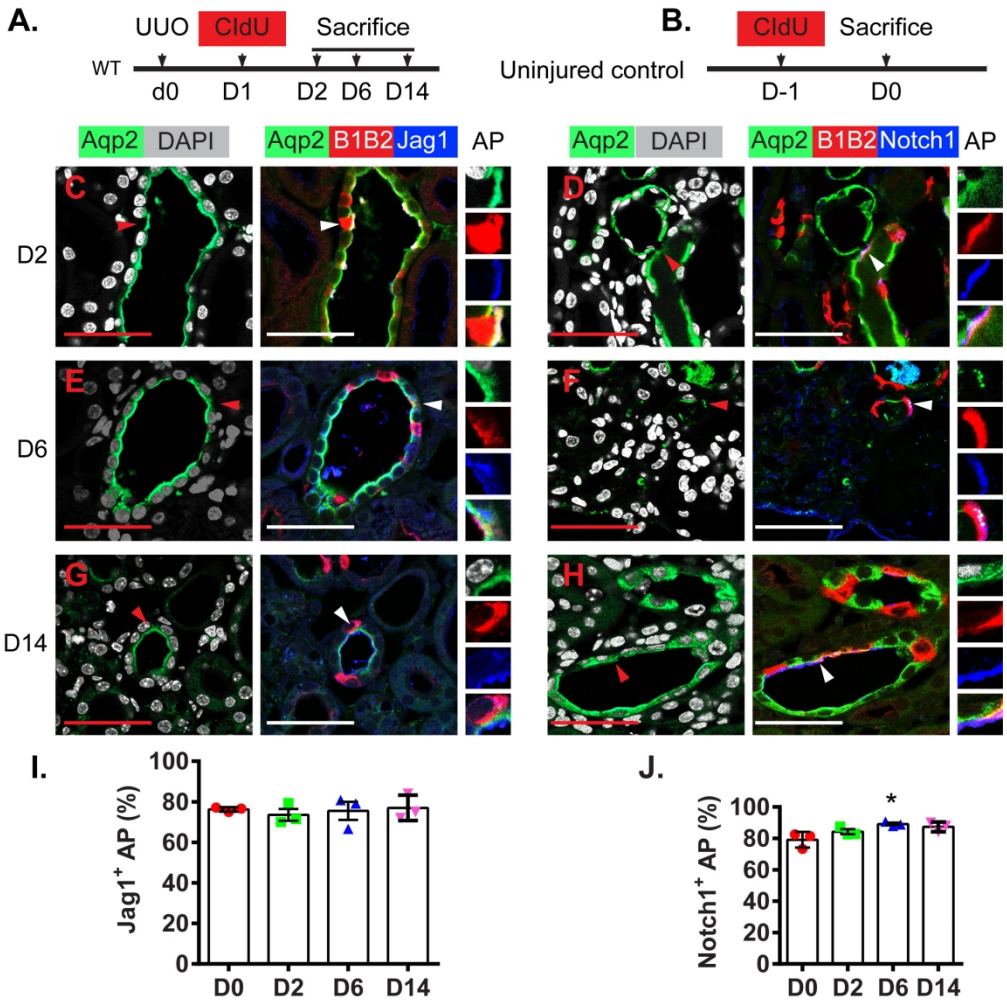

Figure S23. Adult AP express Jag1 and Notch1 during repair.
(A) Adult mice were subject to UUO at day 0 (d0), CldU injection at day 1 (D1), and examined 2, 6 or 14 days later (D2, D6, or D14).
(B) Mice were injected with CIdU and sacrificed one day later as non-injured control (D0).
(C-H) Immunofluorescence images of UUO kidneys showing Aqp2 (green) merged with DAPI (white), or with B1B2 (red) and Jag1 or Notch1 (blue) as indicated. Arrowheads: AP (Aqp2+ B1B2+) were magnified 2.3X on the far right.
(C, E, G) AP expressed high levels of Jag1.
(D, F, H) AP expressed high levels of Notch1.
(I-J) Percent of AP expressing Jag1 (I) or Notch1 (J) in all AP at each time point. About 300 AP were counted per condition. Scale bar: 50 μm. Related to Figure 4 and 7.

201x201mm (300 x 300 DPI)

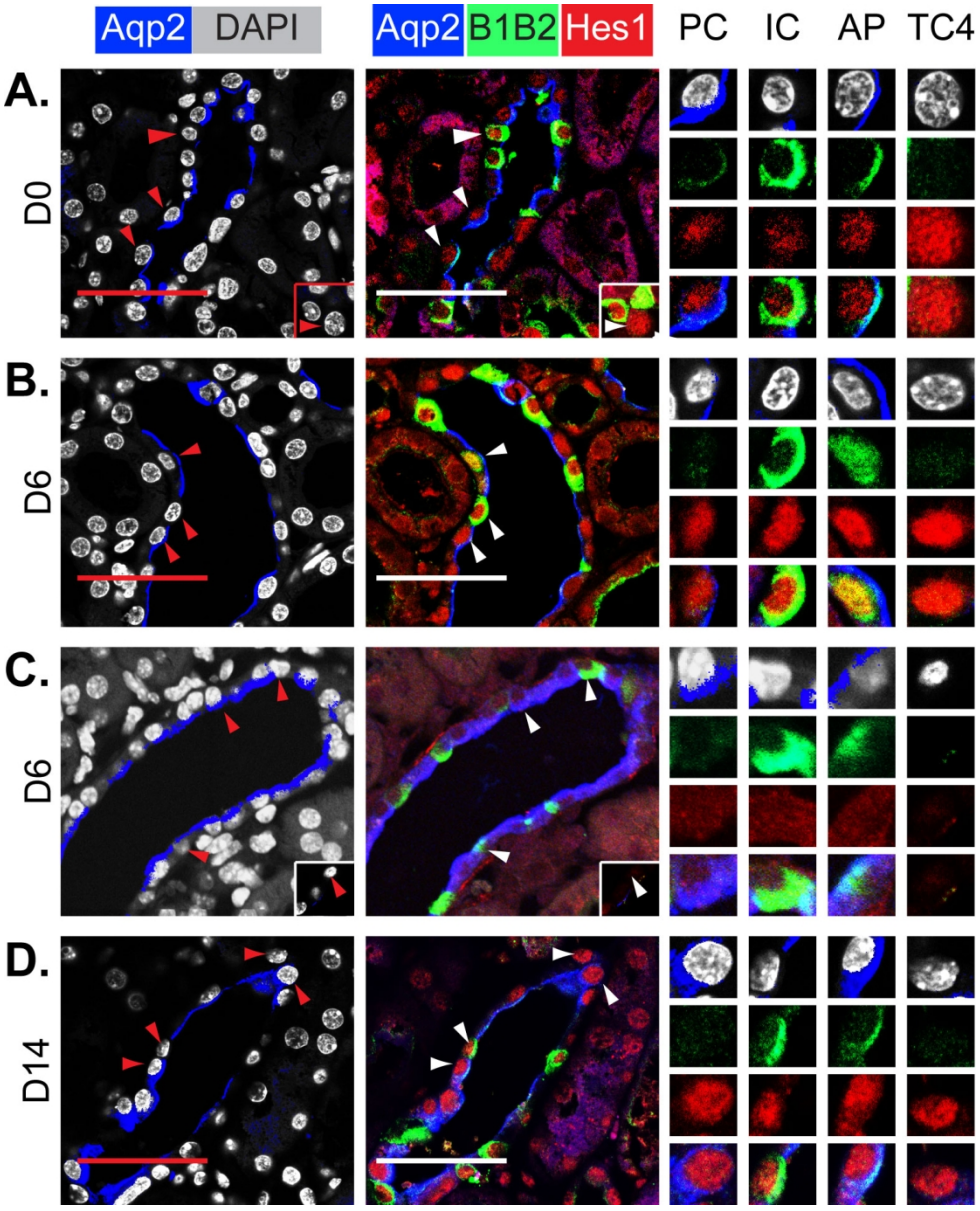

Figure S24. Notch is activated during repair.
(A-D) Images of Aqp2 (blue) merged with DAPI (white, left), or with B1B2 (green) and Hes1 (red, right) in UUO kidneys at D0, D6 and D14. Inserts in A and C were from different microscopic fields. Arrowheads: Hes1-expressing PC (Aqp2+ B1B2-), IC (Aqp2- B1B2+), AP (Aqp2+ B1B2+) and TC4 (Aqp2- B1B2-) were magnified 2.3X on the far right, with split channels. Note, no cells in the CNT/CD in C had detectable Hes1 expression. Scale bar: 50 μm. Related to Figure 7.

131x162mm (300 x 300 DPI)

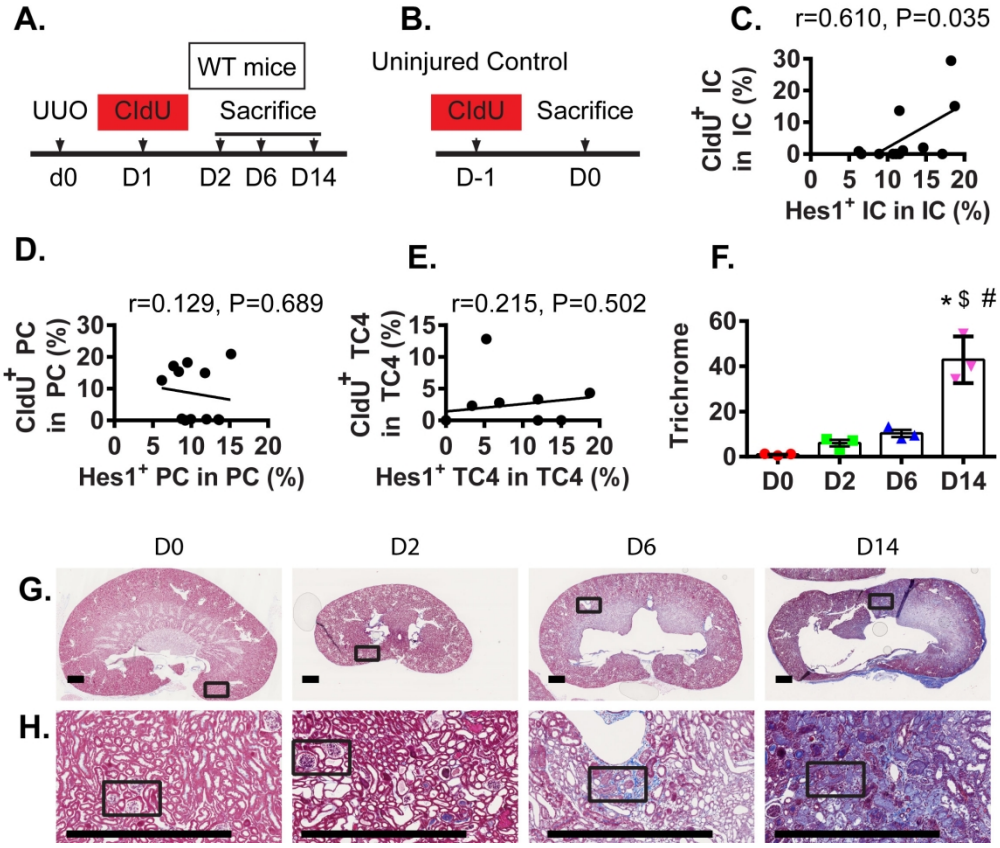

Figure S25. UUO progressively induces kidney fibrosis.
(A) Adult mice were subject to UUO at day 0 (d0), CldU injection at day 1 (D1), and examined 2, 6 or 14 days later (D2, D6, or D14).
(B) Mice were injected with CIdU and sacrificed one day later as non-injured control (D0).
(C-E) Correlation analyses between the percent of Hes1+ cells and percent of CIdU+ cells in all IC (Aqp2- B1B2+) (C), PC (Aqp2+ B1B2-) (D), and TC4 (Aqp2- B1B2-) (E). Each data point represents an individual mouse in which the correlated parameters were analyzed. A total of 8-11 mice from D0, D2, D6 and D14 post UUO (n=2-3 mice/time point) were shown.
(F-H) ImageJ-based quantification of Masson's Trichrome staining (F) and representative Masson's Trichrome staining images (G-H) showing progressive development of severe kidney fibrosis by D14 after UUO. Boxed areas in G were magnified 10X in H. Boxed areas in H were magnified 4X in Figure 7H. Scale bar: 1000 μm. n=3 mice per condition. * p< 0.05 vs. D0. $ p< 0.05 vs. D2. # p< 0.05 vs. D6. Related to Figures 4-8.

195x163mm (300 x 300 DPI)